Accepted Manuscript

The Case Against Vast Glaciation in Valles Marineris, Mars

Lucy E. Kissick , Patrice E. Carbonneau
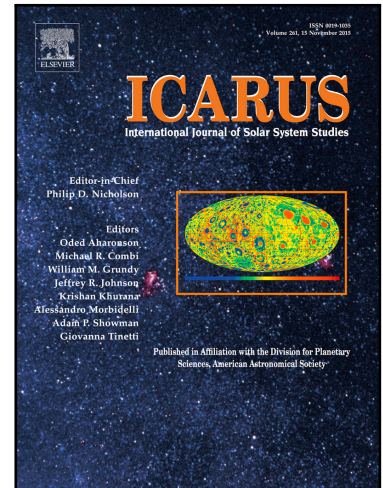
Please cite this article as: Lucy E. Kissick , Patrice E. Carbonneau , The Case Against Vast Glaciation in Valles Marineris, Mars, *Icarus* (2018), doi: https://doi.org/10.1016/j.icarus.2018.12.021

HIGHLIGHTS

- We examine chaos terrain in Valles Marineris and the Chryse Planitia

- We present evidence that chaos terrain is not ice as previously proposed

- Features in Marineris interpreted as glacial do not withstand high resolution scrutiny

- We find no evidence to support the existence of a Marineris glacier, erstwhile or extant

- Groundwater was once present inside Marineris and its discharge created Candor Chaos

The Case Against Vast Glaciation in Valles Marineris, Mars

Lucy E. Kissick[a*, b] and Patrice E. Carbonneau[a]

[a] Department of Geography, Durham University, South Road, Durham, UK.

*lucy.kissick@earth.ox.ac.uk, patrice.carbonneau@durham.ac.uk

[b] Present address: Department of Earth Sciences, University of Oxford, South Parks Road, Oxford, UK.

ABSTRACT

The Valles Marineris of Mars form the largest system of interconnected canyons in the Solar System, where morphological, mineralogical, and structural evidence of widespread glaciation has been recently reported. However, neither precipitation models nor global water budgets can account for such a colossal fill, and the hypothesis has thus far remained unchallenged by additional scrutiny. Here, we present the first thorough case against a Valles Marineris glaciation by describing new evidence that precludes the existence of a glacier. Most crucially, we review High Resolution Imaging Science Experiment (HiRISE) images of chaos terrain in Candor Chasma — previously interpreted as remnant glacial ice — and identify layered, boulder-rich scarps bearing no similarity to scarps of massive ice in Promethei Terra or the North Polar Layered Deposits. We also find no significant differences in the structure, morphology, and composition of chaos terrain in Candor and the Chryse Planitia region, which suggests Candor's

chaos, like Chryse's, is fractured highland terrain. We also review several other key supports for the glacial hypothesis, including the coincidence of an apparent glacial trimline with the water-bearing mineral jarosite, and the apparent presence of glacial features including kettle holes and sandur plains. These too are found to have more plausible explanations with non-glacial origins including tectonic reorganisation, groundwater sapping, and chaotic fracturing. We conclude that the Valles Marineris glacial hypothesis is inconsistent with both observed morphology and our understanding of the ancient Martian climate, and we find no evidence to support its existence.

KEYWORDS

Mars, glacier, Valles Marineris, chaos terrain, geomorphology

1. INTRODUCTION

A school of thought regarding the possibility of a Late Noachian to Late Hesperian (~3.7-3.0 Ga) polythermal glaciation within the Valles Marineris of Mars has emerged over the last decade (Rossi et al., 2000; Thaisen et al., 2008; Fueten et al., 2011; Mège and Bourgeois, 2011; Cull et al., 2014; Gourronc et al., 2014; Makowska et al., 2016; Dębniak et al., 2017). The hypothesis has been fuelled by reported observations of: 1) morphology including ice surface trimlines, deep scour, lateral banks, terminal and ground moraines, outwash plains, patterned ground, truncated spurs, hanging valleys, and hummocky terrain (Fueten et al., 2011; Mège and Bourgeois, 2011; Gourronc et al., 2014; Dębniak et al., 2017); 2) mineralogy including jarosite along the trimline (Cull et al., 2014); and 3) structural reorganisation including crestal ridge slumping and gravitational spreading (Makowska et al., 2016; Mège and Bourgeois, 2011).

However, the precipitation levels required for this voluminous glacier — supposedly

analogous in volume to each Martian pole (Gourronc et al., 2014) — are incompatible with this period's expected cold, arid climate (e.g., Madeleine et al., 2009; Wordsworth et al., 2015). The large flood plains and their associated chaos fields emanating from the system's eastern end imply some groundwater input, but the budget of this is unconstrained (Harrison and Grimm, 2005; Carr and Head, 2015; Grimm et al., 2017). The hypothesis also clashes with widespread evidence within Marineris of lakes of varying size, including aqueously altered mineralogy (Liu and Catalano, 2016), shore-like benches (Harrison and Chapman, 2008), catastrophic spillover routes (Warner et al., 2013), certain analyses of interior layered deposits (Le Deit et al., 2010; Fueten et al., 2014), and subaqueous fans, deltas, and dendritic valleys (Mangold et al., 2004; Quantin et al., 2005; Di Achille et al., 2006; Weitz et al., 2006; Metz et al., 2009). Though such lakes, if they existed, are likely to have frozen solid at some point, most but not all of them (an exception being Warner et al,. 2013) are described as orders of magnitude smaller than the kilometres-thick glacier discussed here.

Multiple claims of glaciation in Marineris have been presented over the past few decades (e.g., Rossi et al., 2000; Chapman et al., 2005) and are over time challenged by alternate explanations (e.g., Warner et al., 2013; Fueten et al., 2014; Okubo, 2016; Rodríguez et al., 2016; Brož et al., 2017). Here, we confront the latest argument for glaciation in Marineris from a geomorphological perspective. We systematically review evidence presented by Gourronc et al. (2014) and others, with particular focus on the reclassification of putative ice-based features as wholly sedimentary based on morphology revealed in high resolution images.

2. VALLES MARINERIS AND THE GLACIAL HYPOTHESIS

Since the first images of a gigantic canyon system on Mars were returned in 1972 by the Mariner

9 mission, Valles Marineris has been a focal point of scientific interest in planetary geography.

Spanning a fifth of the Martian equator and in parts over 10 km deep, it is the largest
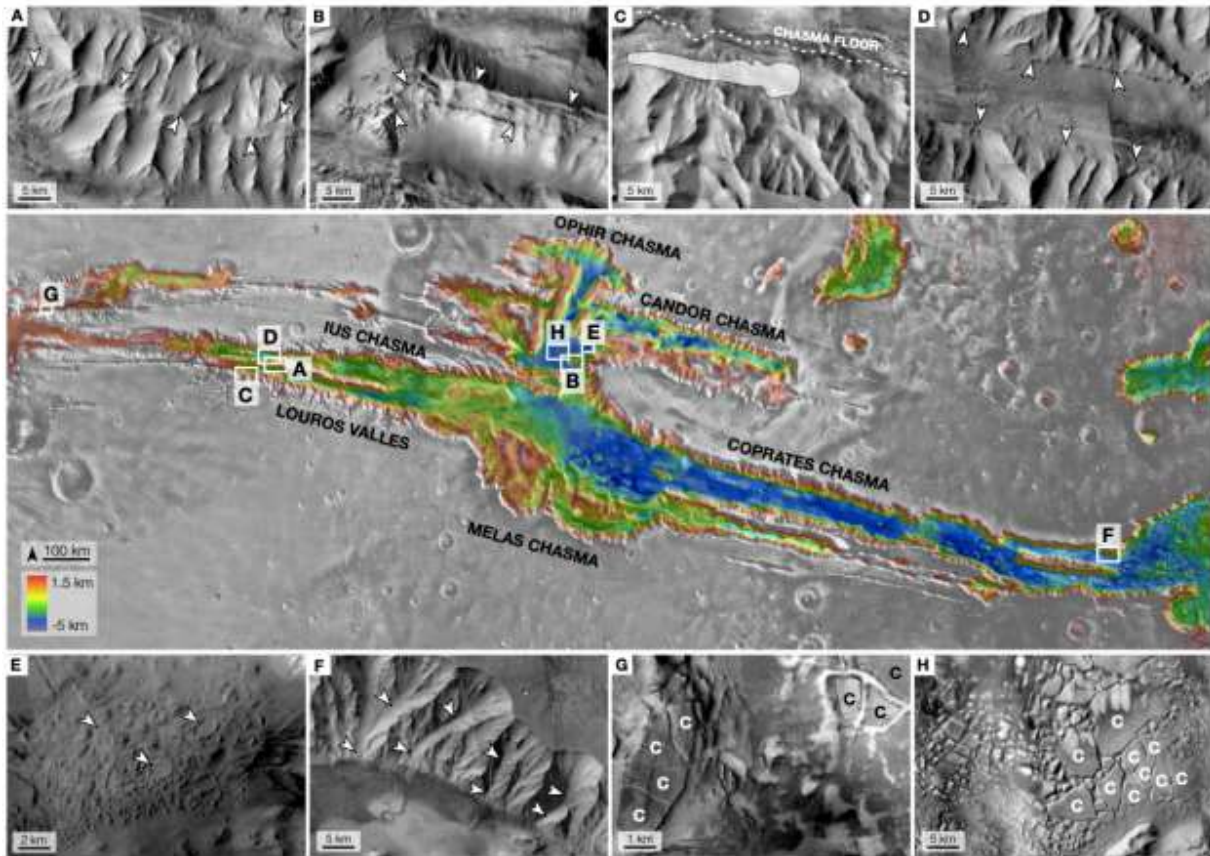
Figure 1 [context map glacial features]. Context map of Valles Marineris with the locations of example features

interpreted as glacial in previous research. The map is a Mars Orbiter Laser Altimeter (MOLA) mosaic atop a

Viking orbital mosaic. Note the same scales excepting *E* and *G*. A) The *sackungen* crestal spreading feature of Ius

Chasma. Note the two roughly-parallel lines following the crest of the ridge, marked with arrowheads. B) Another

prominent example of *sackungen* at the junction between Candor and Melas Chasmata. Here the crestal spreading is

highly pronounced and follows the turns of the ridge. C) The location of the perched jarosite deposit along the wall

of Ius Chasma, marked by the translucent white polygon first demarcated by Cull et al. (2014). The channels of

Louros Valles can just be seen in the lower half of the image, while the chasma floor is marked at the top by the

white dashed line. D) The apparent trimline that continues throughout the Ius-Melas-Coprates and Ophir-Candor

systems as seen in Ius Chasma. This is more closely examined in *Fig. 10*. E) 'Kettle holes' as interpreted by

Gourronc et al. (2014) appear as bright circles, several of which are marked with arrows and are more closely examined in *Fig. 4*. F) A cluster of apparent hanging valleys as designated by Gourronc et al. (2014) that appear random amidst the collapsed walls of the chasma. G) A glacial 'outwash plain' as mapped by Dębniak et al. (2017) at the junction between Noctis Labyrinthus and Ius Chasma, explored further in *Fig. 9*. Blocks labelled *C* are chaotically-organised blocks. H) Candor Chaos in Central Candor Chasma, reinterpreted by Gourronc et al. (2014) as fractured ice. Examples of chaotically-organised blocks are labelled *C*, but the smallest are less than a metre squared and are invisible at this scale. Morphology from MRO CTX images F11_040132_1725_XI_07S082W / B02_010568_1726_XN_07S082W / J04_046356_1730_XN_07S082W (A), P06_003553_1745_XI_05S072W (B) B20_017293_1724_XN_07S083W / J07_047635_1725_XN_07S083W (C), F11_040132_1725_XI_07S082W / B02_010568_1726_XN_07S082W / J04_046356_1730_XN_07S082W (D), HiRISE image ESP_019666_1730 (E), CTX images B17_016303_1649_XN_15S053W / D22_035779_1651_XN_14S052W / F23_044944_1643_XI_15S053W (F) P05_003079_1714_XN_08S091 / J10_048822_1738_XN_06S091W (G), and B18_016686_1738_XI_06S072W (H).

[Two column image, colour should be used. For black and white, topographic colour legend can be removed and image works acceptably in greyscale.]

system of interconnected canyons (or *chasmata*) in the Solar System (McCauley et al., 1972). It strikes northwest-east, beginning from Noctis Labyrinthus on the crest of the Tharsis bulge, spreading to the toe of the Thaumasian Plateau, and opening eastwards into the Chryse Planitia lowlands.

While earlier papers have hypothesised some minor glacial activity in Marineris, inferring features such as *u*-shaped valleys, hanging valleys, arêtes, lateral moraine, ablation moraine, scours, and periglacial-like spur-and-gully morphology (Rossi et al., 2000; Chapman et al., 2005; Thaisen et al., 2008; Mège and Bourgeois, 2011), the idea of major glaciation first gained traction with a chasmata-wide review of apparent glacial morphology by Gourronc et al. (2014). Their research holds that Marineris was entirely glaciated during the Late Noachian to Early

Hesperian, and contained at least 10^6 km^3 of ice in places more than 3 km thick. This is comparable in size to the north and south Martian Poles, at 1.2-1.7 $\times$ 10^6 km^3 and 2-3 $\times$ 10^6 km^3 respectively (Smith et al., 1999). Their stance holds that vast volumes of ice buried by ablation till remain throughout the system, similar to Amazonian-aged debris-covered glaciers (e.g., Shean et al., 2005; Head et al., 2006). From the type of features they identify, including kettle holes and trimlines, the glacier is classed as mostly wet-based — able to flow and slide over its bed with large amounts of liquid water at the base — and its source is given as ice accumulating at low elevation directly from the atmosphere during periods of extreme obliquity.

Three main lines of evidence comprise the Marineris glacial hypothesis and are now briefly summarised with examples and their context displayed in *Fig. 1*.

2.1. Structural evidence

Mège and Bourgeois (2011) note the presence of *sackungen* features (derived from the German *sackung*, or 'slope sagging') throughout Marineris (*Fig. 1a, b*), a term which encompasses gravitational spreading (Varnes et al., 1989) and deep-seated gravitational slope deformation (Dramis and Sorriso-Valvo, 1995). This usually involves mass creep of rock, sometimes along a shear surface, to form crestal grabens and uphill-facing fault scarps along ridge slopes, compensated for by downslope bulging and folding (Bovis and Evans, 1996; Discenza et al., 2011). In Marineris, Mège and Bourgeois (2011) and Makowska et al. (2016) present these features as post-glacial, forming with slope debutressing following a retreating ice mass. Indeed on Earth, *sackungen* features are observed in regions where deglacial unloading and subsequent rebound has occurred in valleys either side (McCalpin and Irvine, 1995; Jarman, 2006), but such features are not exclusively glacial. In fact, they are found frequently on over-steepened slopes

formed by both seismic and aseismic slope reorganisation (Bovis and Evans, 1996; Gutiérrez-Santolalla et al., 2005), often following landsliding events (Johnson and Cotton, 2005), and reflect the general deformation of unsupported valley walls.

The tectonic history of Marineris as a combination of both isostastic and horizontal stress release (Andrews-Hanna, 2012) is consistent with the presence of such crustal spreading features atop the chasmata's most significant grabens (*Fig. 1a* for central Ius and *Fig 1b* for the junction between Candor and Melas). The Marineris *sackungen* is therefore not definitive evidence of glaciation.

2.2. Mineralogical evidence

The presence of jarosite along the wall of Ius Chasma at the 'glacial trimline' elevation has been interpreted as evidence of the Marineris glaciation (Cull et al., 2014; *Fig. 1c*). This mineral forms only under low temperatures and pH (Jamieson et al., 2005) where extremely acidic, evaporating groundwater is inferred to have weathered basaltic rocks, and has been observed across Marineris from Ophir Chasma (Wendt et al., 2011) to Noctis Labyrinthus (Thollot et al., 2012). Cull et al. (2014) argue that the Ius jarosite's odd, perched position along the chasma wall can only be resolved by ice-wall interactions along glacier margins as has been observed on Earth (Lacelle and Léveillé, 2010; Battler et al., 2013).

However, a glacial fill invoked to this level — between -1500 and -2000 m — seems extreme given the assemblage's proximity to the groundwater-sourced channels of Louros Valles. These formed by the sapping of Tharsis-sourced groundwater (Marra et al., 2015) and lead directly into the jarosite region where groundwater was once discharged. Given the widespread coincidence of groundwater and jarosite across Mars, most famously in Meridiani

Planum (e.g., Klingelhöfer et al., 2004; Squyres et al., 2004; Tosca et al., 2005), it is more plausible to consider the Ius jarosite as a spring deposit related to flowing groundwater in this region. This appears particularly likely given the further coincidence of the best-developed sapping channels in Marineris with this best-exposed acidic groundwater indicator. The jarosite could be an indicator of shallower lakes emplaced during the formation of Marineris, perhaps when -1500 to -2000 m represented the base of the system. Either way, kilometre-deep lakes are not necessitated.

Furthermore, sulfates similar to and including jarosite have been found elsewhere across Marineris. These deposits do not follow the 'trimline' and are explained readily by other formation processes, including evaporitic precipitation from water enriched in SO_4 (e.g., Squyres and Knoll, 2005; Roach et al., 2010) or secondary precipitation from groundwater (Gendrin et al., 2005). Most critically in Ophir Chasma, jarosite was also observed at heights of several kilometres upon the chasma walls, but origins from a lake or glacier correspondingly deep was rejected upon the basis that lower elevation sulfate deposits would be far more pervasive under these conditions (Wendt et al., 2011). Secondary precipitation from groundwater, fog, frost, or snow was inferred instead for jarosite formation at this site, but as with the Ius deposit, a perched lake deposit from earlier in the history of Marineris is another possibility (Warner et al., 2011).

The Ius jarosite is therefore also not definitive evidence of widespread glaciation.

2.3. Morphological evidence

A collection of morphological features identified in favour of the Marineris glaciation has been steadily accumulating since the first correlative study by Gourronc et al. (2014), and forms their main line of argument.

A morphological boundary runs throughout the Ius-Melas-Coprates Chasmata system at around -1500 to -2000 m (*Fig. 1d*) and in Candor-Ophir from -4400 to -1600 m, decreasing south into Candor and east to Coprates, beneath which are smoothed, apparently truncated chasma spurs (Chapman et al., 2005; Mège and Bourgeois, 2011). Strata and boundaries in the walls of Marineris have been known since the Mariner missions after which they were named. The 'spurs' have traditionally been considered fault-controlled wall relief (Peulvast and Masson, 1993), while the 'trimline' only described elsewhere as maximum lake level (Harrison and Chapman, 2008) based on the tendency of massifs to display a smooth basal morphology. Gourronc et al. (2014) used the varying elevation of this boundary, its near-continuous presence along wall slopes, and the implication of a general flow direction towards Marineris' eastern opening, to reinterpret it as a glacial trimline. These are weathering limits that mark maximum glacier elevation and require vigorous sliding via basal melt to erode glacially submerged valley walls (Ballantyne, 1997).

Other reported morphologies include a suite of features indicative of basal melt including kettle holes (*Fig. 1e*; Gourronc et al., 2014), and tributary valleys at the putative trimline in Ius and Coprates Chasmata (*Fig. 1f*), which have been interpreted as hanging valleys (Gourronc et al., 2014). The former have been varyingly considered part of the Candor chaotic terrain (Pedersen, 2014) or mud volcanoes (Okubo, 2016), while the latter under the Peulvast and Masson (1993) interpretation were functions of fault-controlled scarping. Most recently, terminal moraines, ground moraines, till plains, and outwash plains were mapped in Ius Chasma, apparently the products of glacial melting in Noctis Labyrinthus to the west (Dębniak et al., 2017; *Fig. 1g*), though no evidence for an original ice body is given and the paper notably lacks any justification for this reasoning.

Cold-based glacial features (glaciers frozen to their beds with diminished erosive capacity) have also been proposed in Marineris: Gourronc et al. (2014) describe lateral moraines along the walls of Ius and Capri Chasma, which represent preserved moraines perched at the ice-wall boundary following deglaciation (Kleman and Hättestrand, 1999). These were first described by Harrison and Chapman (2008) as lacustrine terraces or benches based on their flat-topped profiles and their shared elevation with the 'trimline'. Lateral moraines form from the accumulation of frost-shattered debris and ground wall material, meaning they are poorly consolidated and appear hummocky (Hambrey et al., 1997).

2.4. The 'platy terrain' problem

Gourronc et al. (2014) divide their glacial terrain into three types of increasingly advanced stages as a 'glacial disintegration continuum': 1) *Smooth pitted terrain*, the best-preserved stage, featuring ice beneath veneers of ablation till; 2) *Platy terrain*, characterised by fragmentation of the initial glacier into polygonal blocks, and 3) *Hummocky terrain*, the most advanced and common stage, including mounds, kettle holes, and closed depressions.

Stage 2 of this continuum, the *platy terrain*, offers Candor Chaos (*Fig. 1h*) as the type example of fractured ice. This interpretation deviates significantly from conventional study: chaos terrain is a feature with no terrestrial analogue found almost exclusively within Marineris and the adjacent Chryse Planitia close to the global highland-lowland dichotomy, and is more traditionally described as the surface manifestation of catastrophic eruptions of a fluid, usually groundwater from an overpressured aquifer (see Carr, 1979). It is well-described as rubbly, collapsed assemblages of irregular blocks grading into increasingly degraded buttes, usually angular in plan view and often displaying increased roundness towards site edges or deep regions

of inferred advanced hydrological activity (Chapman and Tanaka, 2002; Rodríguez et al., 2003; Warner et al., 2011; Pederson, 2014). A long-established body of research holds that the onset of the cooler Hesperian era forced kilometre-deep cryospheric extension, pressuring one or more aquifers sufficiently to force breaching along planes of weakness (e.g., faults, impact craters) that are now represented by chaos terrain (Andrews-Hanna and Phillips, 2007; Carr, 1979; Rodríguez et al., 2011). Following loss of subsurface support, fracturing and disintegration occurred with subsidence into the below void, with the expelled fluid eroding the collapsed blocks, smoothening as a continuum from polygonal blocks into knobby terrain (Sharp, 1973; Glotch and Rogers, 2007).

While a variety of alternative triggering mechanisms have been invoked to explain the formation of chaos, including sub-volcanic cryospheric melt (Leask et al., 2006; Zegers et al., 2010), lava dyke collapse (Meresse et al., 2008), and upstream debris flows (Nummedal and Prior, 1981), researchers agree upon the feature being composed of extensionally fractured, cratered highland terrain (e.g., Carr, 1979; Scott and Tanaka, 1986; Rodriguez et al., 2005). There is overwhelming evidence to support this interpretation. Hematite- and sulfate-rich deposits identified by thermal emission, near-infrared, and visible spectroscopy are found interbedded within chaos in Chryse (Gendrin et al., 2005; Glotch and Christensen, 2005; Noe Dobrea, 2006, 2008; Glotch and Rogers, 2007; Lichtenberg et al., 2010). Crucially, extensive correlative and geomorphologic surveys of Iani Chaos show it is composed of remnants of cratered highland terrain with horizontally layered bedrock, often capped by a smooth, resistant unit correlative with that of the surrounding plateau (Warner et al., 2011).

The reinterpretation of Gourronc et al. (2014) that chaos terrain is composed of fractured ice is a serious assumption that requires closer analysis. It is worth noting that chaos terrain is not

confined to the Chryse Planitia: sites are found, for instance, at the head of Dao Vallis along the Hellas impact crater; in the basins of Gorgonum, Atlantis, and Ariadnes in the Eridania region (e.g., Michalski et al., 2017); and associated with the Elysium Montes (e.g., Pedersen and Head, 2011). Were all such terrain composed of ice, the implications for the global climate and water budget of Mars would be of extreme significance.

We here review the chaos terrain/platy terrain problem and other morphology presented as evidence of glaciation including the trimline, spurs, hanging valleys, kettle holes, till plains, outwash plains, and lateral moraines. Our primary aim for this paper is to understand the composition of chaos in interior Marineris as rock in as unambiguous terms as possible, and from there to review the implications of this for the glaciated Marineris hypothesis.

3. STUDY SITE AND METHODS

This paper focuses on Candor Chasma, one of the constituent chasmata of the Marineris system, which is itself a system of seven valleys debouching into a central depression called Candor Chaos. East Candor Chasma is connected to Central Candor by two of these valleys and contains

Chaos terrain	Latitude/ longitude	Average elevation in m	Rough area in km^2	Brief description
Aram	2.6°N, 21.5°W	-2700	56,000	Crater containing broad examples of classic chaos morphology from angular (plan-view) to knobs.

Aureum	3.9°S, 26.9°W	-3200	60,000	Large sub-circular depression, part of the main Chryse chaos system, comprising very well-rounded chaos rafts and knobs.
Hydaspis	3.1°N, 27.1°W	-3400	24,000	Part of the main Chryse chaos system with clear outflow channels, mostly very well-rounded chaos rafts and knobs.
Xanthe Terra crater	1.3°N, 48.5°W	-200	2,000	Confined to two overlapping craters, separate from the main Chryse chaos system, no outflows, defined by highly angular fractures grading to knobs with little rounded intermediates.
Central Candor	6.9°S, 72.5°W	-4600	5,000	Relatively angular in plan view, large blocks confined to the chasma

|				floor in Central Candor Chasma, characterised by blocks becoming increasingly smaller and rounder at terrain's outskirts where ringed ridges appear.
Major East Candor	6.2°S, 70°W	-4800	400	Very well-rounded chaos blocks, interspersed with ringed ridges, confined to East Candor Chasma floor.
Nia	6.7°S, 67°W	-4700	550	Very angular chaos blocks, confined to East Candor Chasma floor, no ringed ridges or rounded knobs.
Minor East Candor	6.3°S, 70°W	-4800	18	Very well-rounded chaos blocks, very small and isolated instance, interspersed with ringed ridges, connected to Major East Candor

				Chaos by dendritic channels.

Table 1. Basic statistics and a description for each chaos terrain studied in this paper for reference.

[One or two column figure.]

three additional, minor chaos fields. While Central Candor Chaos has been mentioned in one or two earlier studies (Lucchitta, 1999; Okubo, 2016), and one of these minor sites has recently been named Nia Chaos after a mapping project by Okubo and Gaither (2017), the two other instances in East Candor are, to the authors' knowledge, formerly undescribed.

We use Mars Reconnaissance Orbiter Context Camera (CTX) images at 6 m pixel[-1] resolution, and High Resolution Image Science Experiment (HiRISE) images at 25 cm pixel[-1] where available, to conduct a simple, in-depth morphological study of the chaos polygons within Central and East Candor. All images were obtained from the NASA Planetary Data System and imported into the GIS software package ESRI ArcMap. Four chaos terrain sites from the Chryse Planitia region are also analysed for comparison with Candor, since all chaos terrain differs slightly based on: rock type, level of hydrologic alteration, number of reactivation events, age, proximity to other chaos sites, etc. (see Warner et al., 2011, for an in-depth descriptive study). The chaos terrain of Aram, Aureum, Hydaspis, and an unnamed crater in Xanthe Terra are selected based on their slightly-differing geomorphology: e.g., the chaos in Aram is typically more angular in plan view than that of Aureum, and while the chaos in Hydaspis is part of a wider system, chaos in the Xanthe Terra crater is isolated and does not contain
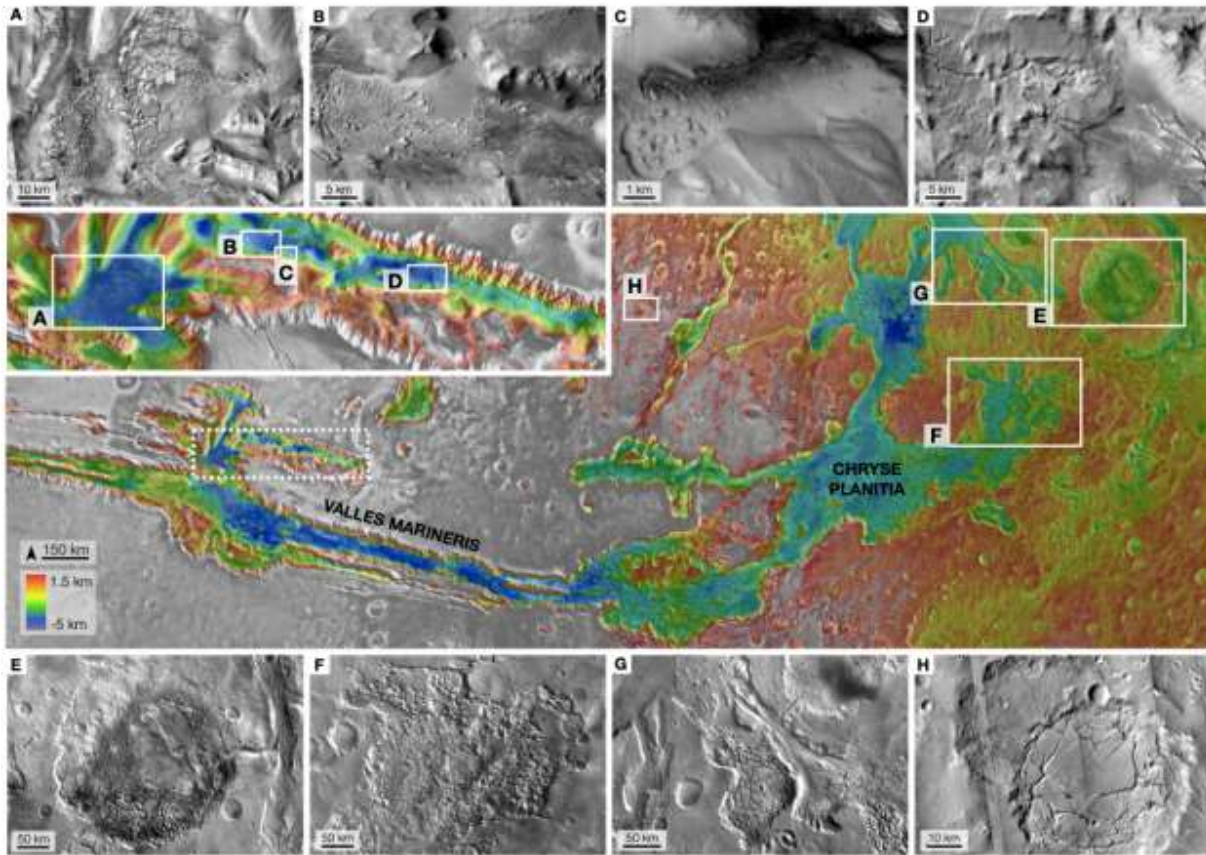
Figure 2 [context map chaos terrain]. Context map of Valles Marineris and its relationship with the circum-Chryse Planitia chaos terrain. The map is a Mars Orbiter Laser Altimeter (MOLA) mosaic atop a Viking orbital mosaic. Take care to note varying scales, and Central and East Candor inset to the left. A) Central Candor Chaos (known in the literature as Candor Chaos) with its angular-edged chaotic blocks. B) Major East Candor Chaos. C) Minor East Candor Chaos, tenuously connected to Major by dentritic channel-like structures. D) Nia Chaos. E) Aram Chaos and its outlet to Ares Vallis. F) Aureum Chaos. G) Hydaspis Chaos located lower center, with clear outflow channels to the Simud-Tiu Valles. H) The unnamed Xanthe Terra crater located between the Shalbatana and Hypanis Valles.

[Two column image, colour should be used. For black and white, topographic colour legend can be removed and image works acceptably in greyscale.]

discernible outflow channels. Most of these sites have been previously studied (e.g., Rodríguez

et al., 2004; Glotch and Christensen, 2005; Glotch and Rogers, 2007; Spagnuolo et al., 2011; Sowe et al., 2012; Roda et al., 2014, 2015; Coleman, 2015). Basic statistics and descriptions for each site in Marineris and Chryse can be found in *Table 1*.

The criteria used to identify chaos have been well-established in works such as Sharp (1973), Andrews-Hanna and Phillips (2007) and Warner et al. (2011). Sharp et al. (1971) were the first to recognise this terrain in the Mariner 6 flyby, with Sharp (1973) using the more detailed Mariner 9 imagery to describe it as assemblages of polygonal, irregular-shaped blocks up to tens of kilometres across, with arc-shaped slump blocks on bounding escarpments. They are divided by linear fractures and occupy lowlands or depressions within the relatively older cratered uplands, showing preserved remnants of this terrain on the surface. In Central and East Candor, chaos blocks are distinguishable from non-fractured surroundings by the following: striking angularity; steeply raised, flat-surfaced plateaus; deep intervening cracks; and their location in open, flat regions of the chasma floor.

Chaos blocks often grade into increasingly separate, smoothed, conical mounds and eventually into knobby terrain, so called because of its appearance as vast fields of knob-shaped buttes. These are distinguishable by their fretted appearance, smoothed intervening troughs, and systematic association with polygonal blocks. In these degraded regions, sub-circular to elongate, ringed hollows have been previously described (Gourronc et al., 2014; Okubo, 2016). These are mapped by identification of raised, narrow, generally discontinuous rims, on average 1-3 km at their longest axis, usually with flat, smoothed interiors, and their tendency to associate in clusters at the margins of major chaos terrain.

Given the exceptional variety of morphology within individual chaos terrains, four forms of chaos morphology were selected to study within each site: 1) chaos of exceptional angularity

in plan view; 2) chaos of exceptional roundness; 3) degraded knobs (knobby terrain); and 4) regions where 1-3 form a continuum from angular to degraded knobs. The cause of this continuum has often been speculated upon: blocks may become increasingly degraded with increasing water activity, or perhaps as a function of the initial density and depth of fracturing, followed by scarp backwasting and slope replacement (e.g., Warner et al., 2011).

We also examine additional 'glacial' features with HiRISE resolution where possible, comparing the morphology of features such as the 'outwash plains' of Ius Chasma, the 'trimline' from Coprates-Ius, and the 'lateral moraines' of Ius and Coprates to descriptions of their terrestrial equivalents, alongside compiling observations and descriptions of their apparent Martian equivalents in Marineris at the CTX and HiRISE scale. We particularly seek to identify distinctive characteristics belonging to these features on Earth to provide reasoning behind their presence or absence in this chasma; such characteristics are discussed in detail alongside descriptions of the features in Marineris.

Lastly, we conduct more quantitative studies on the composition of the terrain itself to better understand whether it is ice or rock. This is critical in assessing the validity of the glacial Marineris hypothesis, with the 'platy terrain' of Candor offered as a key line of evidence supporting the notion of vast swathes of buried ice across the chasma. Our analysis here includes HiRISE comparison of typical ice-based and rock-based terrains, the ubiquity of boulders at such sites; the preservation potential, longevity, and morphology of craters in these terrains; and general characteristics of these terrains of such vastly different composition. We also create slope profiles for known ice-based terrain (the Polar Layered Deposits), known rock-based terrain (chaos of the Chryse Planitia), and for mesas in Candor Chaos, to provide a degree of quantification of their slope curvatures.

4. RESULTS: THE MORPHOLOGICAL STUDY

We describe first our morphological study of the Marineris chaos in Central and East Candor, followed briefly by the morphology of the Chryse chaos in Aram, Aureum, Hydaspis, and the Xanthe Terra crater. The context for all six sites is given in *Fig. 2*, and example morphology from each site of the four terrain types studied is displayed in *Fig. 3*. The specific locations of these examples can be found in the Supplementary Figures (S1).
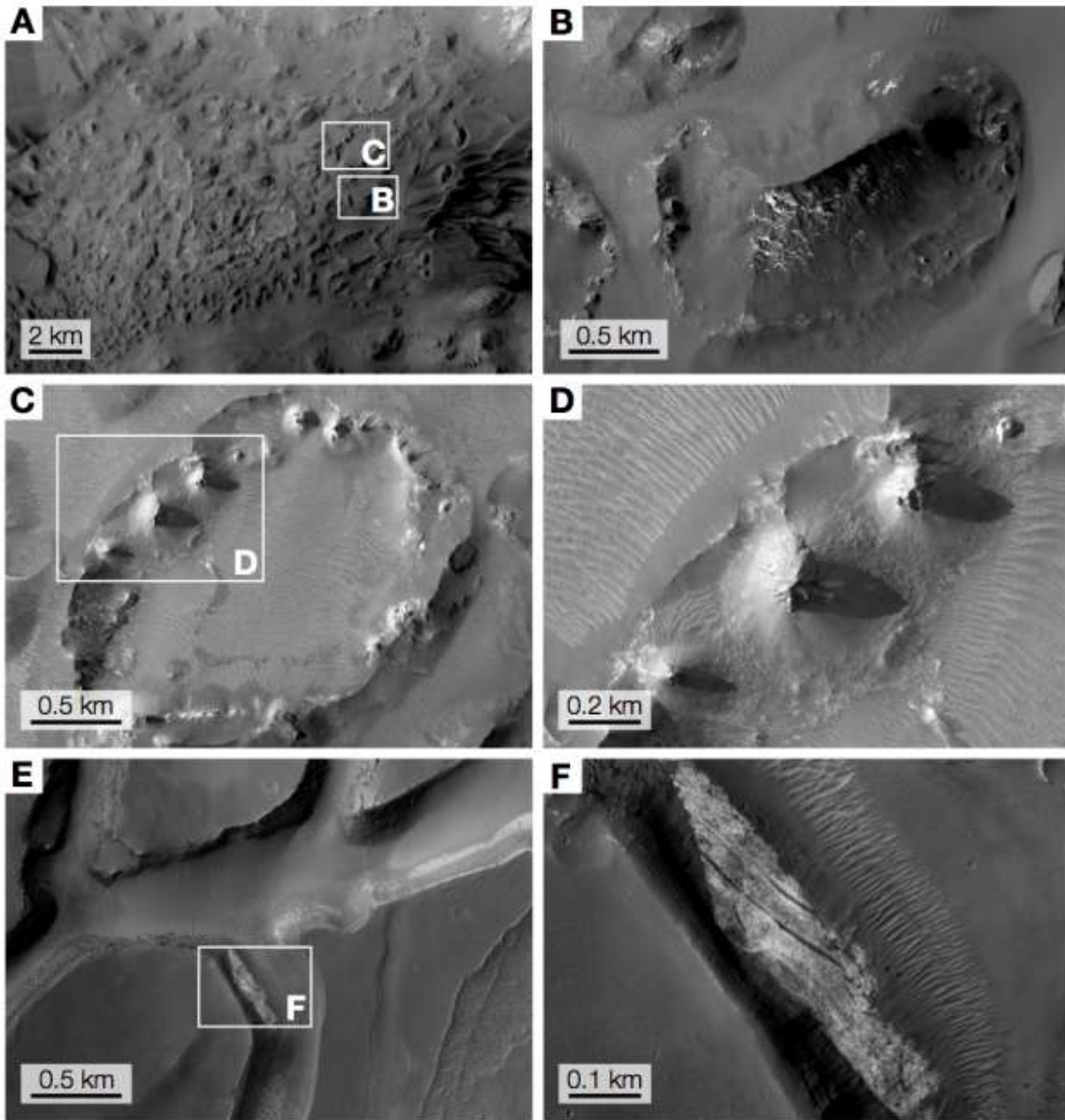
4.1. Candor Chaos

4.1.1. Central Candor Chaos

Located in the centre of the Candor Chasmata system, Central Candor's chaos in *Fig. 2a* has clearly defined margins that extend north, where it transitions to rubbly blocks. Chaos mounds are mostly flat-topped and angular in plan view (*Fig. 3*, see *Central Candor: angular*), ranging in size from over one hundred kilometres to minute, conical mounds (*Fig. 3*, see *Central Candor: knobby*). They often demonstrate pre-chaos alignment between fractures, marking transition from unaltered to fractured surfaces (*Fig. 3*, lower right of *Central Candor: angular*), and become increasingly rounded and smaller to the southwest (*Fig. 3*, *Central Candor: rounded* and *knobby*).
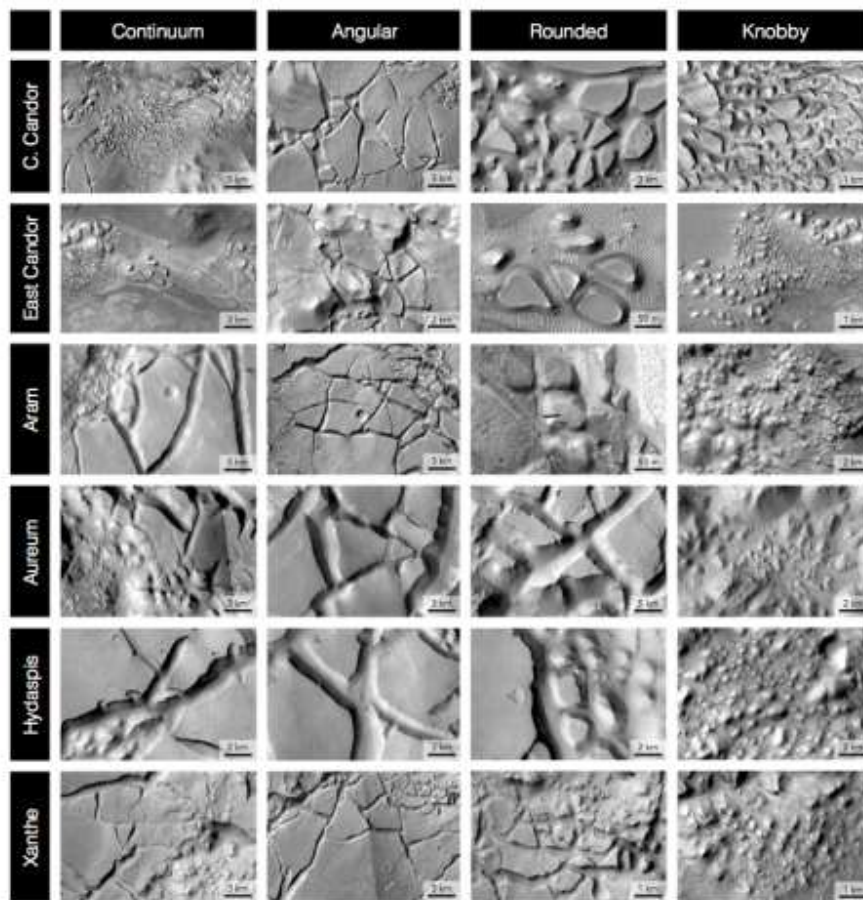
Figure 3 [morphology grid]. A grid of the four forms of chaos morphology selected for study within each site, which represent the diversity of chaos terrain morphology. Left to right: regions of a continuum from angular to degraded knobs; chaos of exceptional angularity in plan view; chaos of exceptional roundness; and degraded knobs (also known as knobby terrain). Examples of these terrain are selected from each of the sites studied, with the three sites in East Candor collected in one category given their relatively small areas. Top to bottom: Examples of morphology from Central Candor; East Candor (Major, Minor, and Nia); Aram; Aureum; Hydaspis; and the Xanthe Terra crater. Note the varying scales. Specific locations and the ID numbers of the CTX images used are noted in the Supplementary Figures (S1).

[Two column image, black and white.]

Figure 4 [ringed ridges]. The ringed ridges of Candor Chasma, interpreted as kame and kettle holes by Gourronc et al. (2014), with examples from Central Candor Chaos. A) Context for subsequent close-ups, where at least a dozen other ringed ridges may be discerned. B) An infilled ringed ridge, interpreted as a degraded chaos block that is preferentially eroding inwards to leave its more competent outer rim. C) A ringed ridge, interpreted as a more advanced stage than *4b* whereby the original inside chaos block has eroded away. D) Close-up of the ring in *4c*. The individual cone-shaped mounds that comprise parts of the ring led Okubo (2016) to conclude they are mud volcanoes, but the rest of the ring appears continuous rather than in discrete cones. Boulders can be seen in relation

to the ridge's slopes. Morphology for A-D from HiRISE image ESP_019666_1730. E) Possible outcrops of interior layered deposits from within chaos rafts in Nia Chaos, East Candor. (F) A close-up of the bright outcrop in Nia Chaos. HiRISE image for E and F is ESP_042940_1735.

[One or one point five column image, black and white.]

Elliptical to circular hollows are, to the authors' knowledge, only found in the Central and East Candor Chasmata, and here they tend to cluster in narrow valleys (*Fig. 4a*). Closer inspection reveals they are not depressions but composed of discontinuous ridges. A clear evolution from degraded mounds (*Fig. 4b*) into the rings (*Fig. 4c*) that eventually disintegrate to boulders (*Fig. 4d*) may be observed, with disintegration seemingly growing as a central depression until only the original perimeter is left as a ringing ridge. In *Fig. 4e* and close-up in *4f*, possible outcrops of bright, interior layered deposits, which are primarily mono- and polyhydrated sulfates, can be seen within chaos rafts in Nia Chaos, East Candor. This rock type could explain why the ringed ridges apparently – to the authors' knowledge and following extensive searching – form solely in Central Candor and East Candor.

4.1.2. East Candor Chaos

Three distinct chaos terrains are studied in East Candor. The most westerly is a quasi-linear basin (*Fig. 2b*), here named for simplicity Major East Candor Chaos, which contrary to its larger neighbor in Central Candor comprises chaos as mostly well-rounded mounds (*Fig. 3*, see *East Candor: rounded* and *knobby*). To the south and southeast in particular, they transition from angular in plan view to very small and ill-defined knobs (*Fig. 3*, *East Candor: continuum*). Ringed ridges, unlike in Central Candor where they are confined to one region, are dispersed throughout the chaos.

Located immediately southeast of the westerly chaos is one of the deepest chaos terrains on Mars, here named Minor East Candor Chaos (*Fig. 2c*). In many respects it displays classic chaos style: a clearly defined, steep-sided basin filled with rubbly, rounded blocks; a direction of outflow indicated by a tapering-out 'tail'; even a potential inlet channel to the northwest where it connects with Major East Candor Chaos. Several ringed ridges are scattered throughout the chaos.

In *Fig. 2d* is the most easterly chaos in East Candor, recently named Nia Chaos after its association with the adjacent Nia Mensa, and is also a quasi-linear basin of west-east strike. Its blocks are angular in plan view and large (*Fig. 3*, see *East Candor: angular*), with shallow intervening fractures often displaying scree slopes of loose sediment (*Fig. 3*, *East Candor: boulders*). There are no visible circular ridges, and no instances of rounded or knobby terrain.

4.2. Chryse Chaos

The Chryse Planitia is a roughly circular depression into which the scars of the largest overland flow channels in the Solar System debouch, including the major valles of Kasei, Maja, Shalbatana, Simud, Tiu, and Ares. These channels are sometimes sourced from notched headlands (e.g., Echus Chasma for Kasei Vallis) but usually emanate from chaos terrain, as in the cases of the largest excluding Kasei, including Maja Vallis from Juventae Chaos, Ares Vallis from Iani and Aram Chaos, and the Simud-Tiu Valles from a vast, interconnected system that includes the Aureum, Eos, Hydaspis, and Hydraotes Chaos. While chaos terrain exists in regions outside of Chryse, such as Atlantis, Gorgonum, and Ariadnes Chaos in Eridania, and at the heads of the Niger and Dao Valles in the Hellas impact crater, the vast majority is confined to the circum-Chryse region.

The first three sites now discussed are exemplar chaos terrain based on their systematic association with outflow channels and their already well-described morphologies, while one example (the unnamed crater in Xanthe Terra) deviates from this standard and is here included as an example of atypical chaos. They are all here briefly described for comparison with the Candor chaos.

4.2.1. Aram Chaos

Aram Chaos is located in Aram Crater (*Fig. 2e*) and is one of the most classic examples of chaos terrain: it demonstrates a clear continuum from angular chaos in sharply fractured terrain in higher ground (*Fig. 3*, *Aram: continuum* and *angular*), progressively better rounded in lower terrain, eventually forming minute knobs near a break in the crater rim (*Fig. 3*, *Aram: rounded* and *knobby*), where the scour of an ancient outflow channel can clearly be seen joining with Ares Vallis. Typical chaos terrain from angular to rounded morphology are clearly displayed at this site.

4.2.2. Aureum Chaos

The chaos in Aureum (*Fig. 2f*) occupies a depression linked to the main Chryse chaos region and comprises exceptionally rounded chaos blocks in plan view: even the most angular in plan view sections found are smooth-cornered and separated by deep gullies (*Fig. 3*, compare *Aureum: angular* with *Aureum: rounded*, and note the little difference). Some parts of the chaos basin are smoothed clean even of knobby terrain and are flat, featureless clearings.

4.2.3. Hydaspis Chaos

Hydaspis Chaos (*Fig. 2g*), like Aureum, is located deep within the main Chryse chaos region but further downgradient where the telltale scour and flutings of outflow channels are more prominent. The morphology of Hydaspis Chaos is also similar to Aureum in that angular terrain is difficult to come by (*Fig. 3*, compare *Hydaspis: angular* with *Hydaspis: rounded*), and similarly the two have clear outflow directions through which water exited the system.

4.2.4. Xanthe Terra crater chaos

Located between the heads of the two major valles Shalbatana and Hypanis, this unnamed crater system (*Fig. 2h*) is separate from the main Chryse chaos region and its chaos is confined within two overlapping craters as jagged, poorly developed fractures. Contrary to Aureum and Hydaspis, chaos terrain here is exceptionally angular when viewed in plan, and rounded terrain is difficult to come by (*Fig. 3*, compare *Xanthe: angular* with *Xanthe: rounded*), and there are no outflow channels. The site shows the characteristic continuum from angular to knobby terrain.

At all four sites, HiRISE-scale inspection of the block sides reveals boulders tumbling from distinct horizons that appear to differentially weather to produce protruding strata.

5. MORPHOLOGICAL COMPARISON INFERENCES

Our results show the candidate chaotic terrain in Central and East Candor is morphologically indistinguishable from the reference chaos in the circum-Chryse region. Several lines of reasoning lead to this conclusion:

Firstly: the continuum of transition from angular, shallowly fractured terrain, to conical mounds, to sparse knobs, is characteristic of chaos terrain and is demonstrated in both Central and East Candor. *Fig. 5* shows the highlights from *Fig. 3* to reveal the most striking instances of

similarity between the Candor (left) and Chryse (right) terrain at identical scales. The two figures together show how all sites demonstrate the varying morphology of chaos terrain across all five criteria studied (*continuum*, *angular*, *rounded*, *knobby*, and *boulders*).

Secondly, the 'kames' and 'hummocky terrain' as described by Gourronc et al. (2014), are revealed by HiRISE as rings of ridges or loose mounds that appear to grade from heavily-eroded chaos knobs into hollowed-out rings (*Fig. 4*). These ringed ridges appear remarkably similar to the knobby terrain shown in *Fig. 5g* and *h*, though with hollow interiors and a prominent ring around their outsides. *Fig. 4c*, which we interpret to be a further eroded example, shows only this ring remaining, and is here interpreted as an extreme chaos disintegration feature indicative of groundwater outflow erosion, where chaos blocks have begun to erode from the inside out. The exact mechanism by how this forms is unclear as these ringed ridges are only found in association with Candor Chaos, and are perhaps a result of the local rock type: the interior layered deposits of Marineris, as they are known, are rhythmically bedded, sulfate-rich sequences of sediment found in kilometre-high mesas within Candor Chasma and in smaller outcrops throughout Marineris. These outcrop brightly in CTX and HiRISE images, appearing to weather competently (Okubo and McEwen, 2007), and are possibly eroding from within chaos blocks in Nia Chaos (*Fig. 4e*, with detail in *4f*). The ringed ridges of Central and East Candor share this brightness and competence, which could imply the same rock type and explain their exclusivity to interior Marineris. Alternatively, Okubo (2016) interpret the exact examples shown in *Fig. 4c* as evidence of mud volcanism based on their small cone shapes with summit depressions. With either interpretation, chasmata-wide glaciation is not necessitated, both alternatively implying some mobilisation of subsurface sediments and fluids.

Several other lines of evidence leading to this conclusion and are now explored in depth.
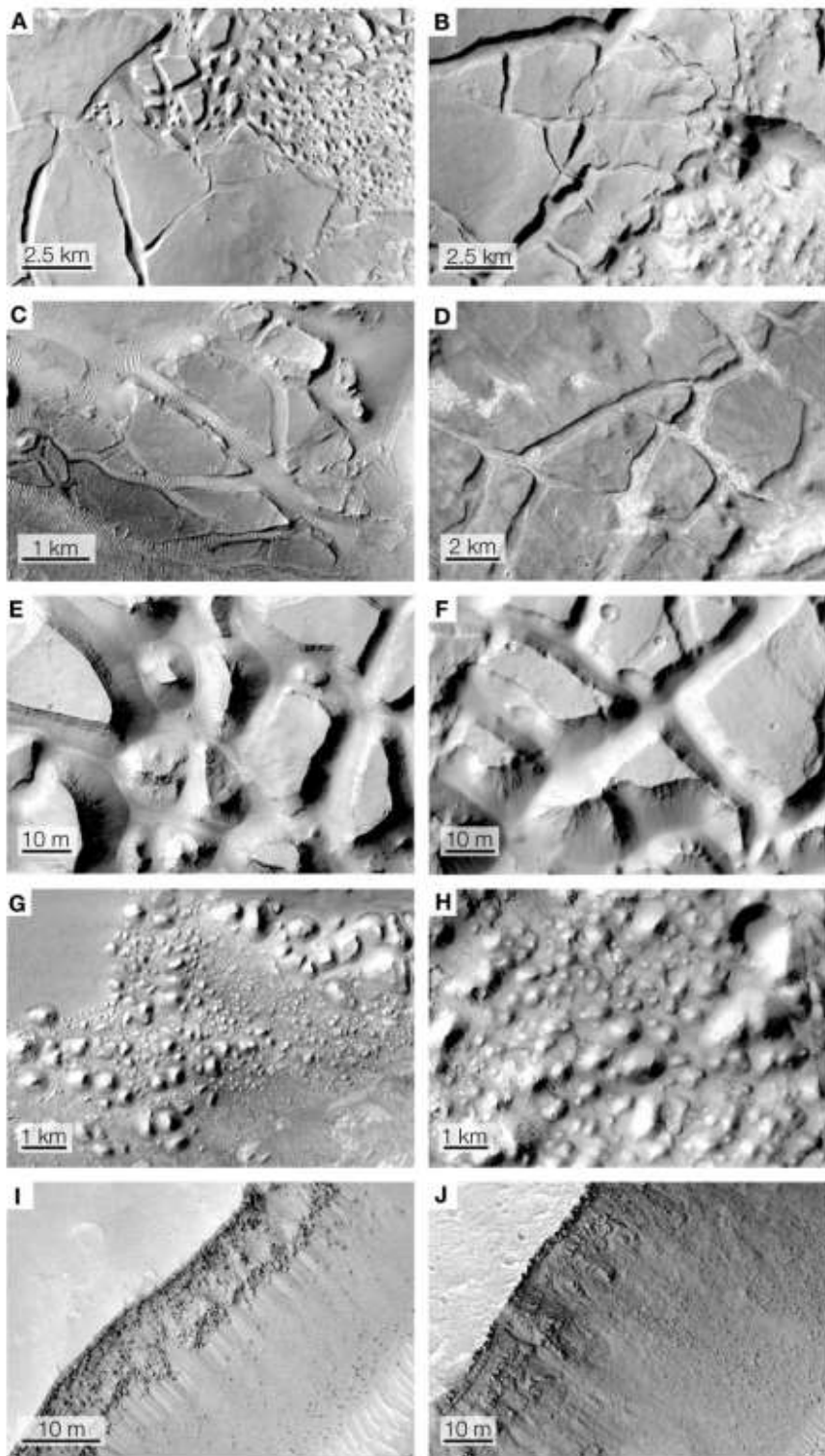
Figure 5 [exemplar morphology]. Exceptional examples of candidate chaos morphology in the left column from

Central and East Candor's chasmata, compared with the right column's typical Chryse Planitia chaos with examples

from Aram, Aureum, Hydaspis, and the unnamed Xanthe Terra crater. Note the often-similar scales. A) A continuum from angular to rounded chaos in Candor. B) Comparable continuum in Xanthe Terra. C) Angular chaos in East Candor. D) Comparable angular chaos in Aram. E) Rounded chaos in Candor. F) Comparable rounded chaos in Aureum. G) Knobby terrain in Candor. H) Comparable knobby terrain in Hydaspis. I) Close-up of the sides of candidate chaos rafts in Candor; note the tumbling boulders and distinct strata. J) Comparable close-up of the sides of chaos rafts in Hydaspis, also with boulders. Morphology from MRO CTX images P06_003553_1745_XI_05S072W (A), B17_016395_1793_XN_00S048W (B), P01_001522_1734_XN_06S069W (C), B19_017172_1828_XN_02N020W (D), B18_016686_1738_XI_06S072W (E), P02_001969_1761_XN_03S027W (F), P01_001522_1734_XN_06S069W (G), D02_028117_1854_XI_05N020W (H), and HiRISE images ESP_040369_1730_RED (I), and PSP_003314_1825_RED (J).

[One to one point five column image, black and white.]

5.1. Rock or ice? The HiRISE study

In all sites, HiRISE-scale inspection of the block sides reveals boulders tumbling from distinct horizons that appear to differentially weather to produce proud strata (*Fig. 5i, j*). Whether these are rock or ice is critical information now explored.
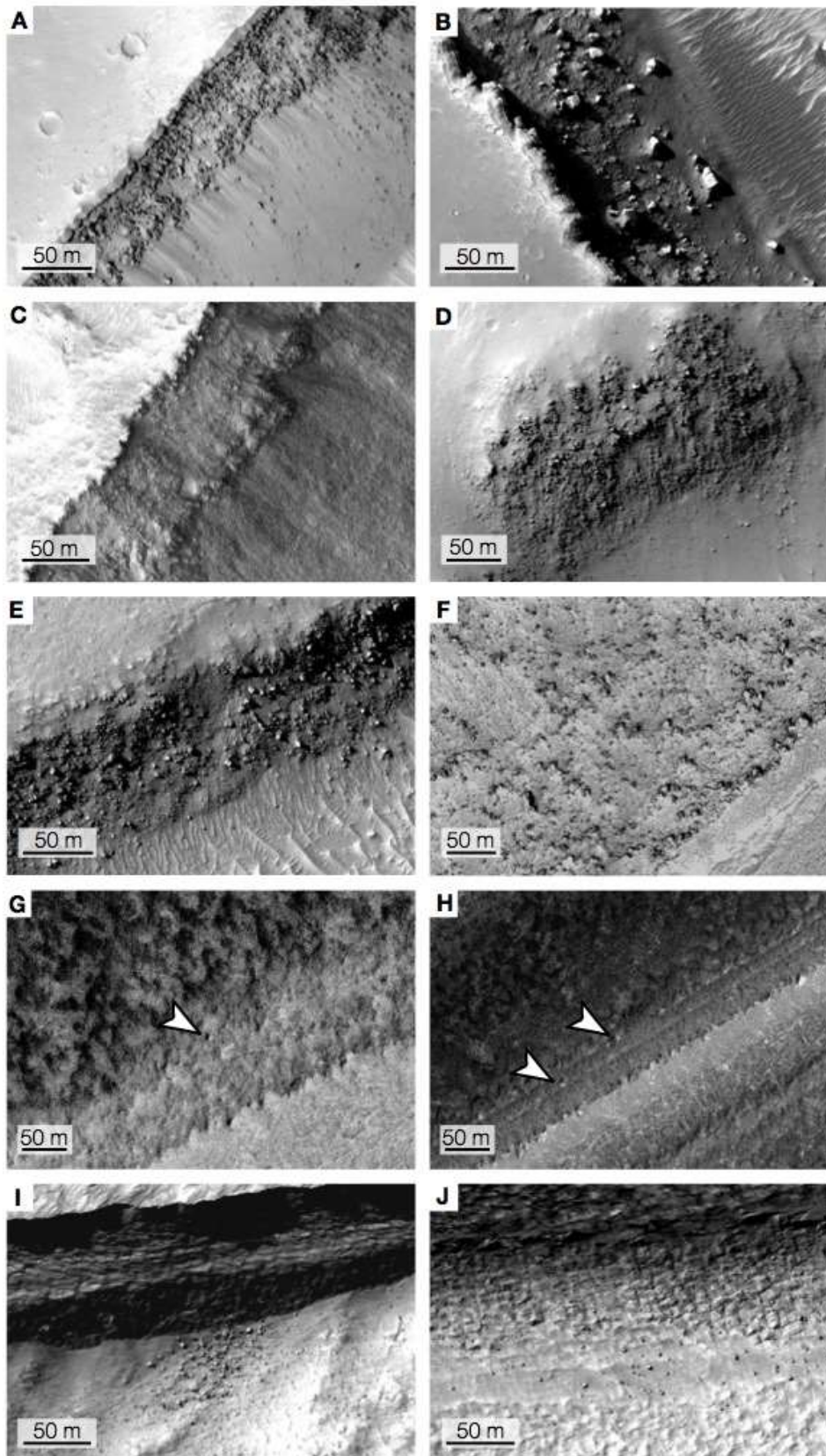
Figure 6 [boulder morphology]. Examples of boulder morphology and abundance, which can be used to gain an insight into the fundamental structure and composition of a terrain. Two examples are given each from Candor (including Central, Major East, Minor East, and Nia; A and B), Chryse (including Aram, Aureum, Hydaspis, and the Xanthe Terra crater; C and D), the highlands surrounding the chaos terrain (E and F), the Polar Layered Deposits (G and H), and the massive ice scarps identified by Dundas et al. (2018; I and J). A) Boulders on a scarp in Central Candor. B) Boulders on a scarp in Nia Chaos, East Candor. C) A scarp in Hydaspis Chaos. D) Boulders on a scarp in Aureum Chaos. E) A boulder-rich scarp in the highlands south of Aureum Chaos. F) Boulder-rich scarp in the highlands adjacent to Ophir Chasma. G) Boulder-scarce polar layered deposit slope; arrows denote one potential instance of a lone boulder. H) Boulder-scarce Polar Layered Deposit (PLD) slope, with arrows denoting potential boulders. Boulders were extremely uncommon in all images of the PLD searched; these were the two best examples identified. I) A massive ice scarp identified by Dundas et al. (2018) in Promethei Terra. Note the abundance of boulders only associated with a darker lens in the section; this is a rocky inclusion that was not identified elsewhere, and the boulders are only associated with this section. No calved ice or ice boulders were found. J) Another instance of boulders associated with the previous example in Promethei Terra identified by Dundas et al. (2018). All image ID numbers can be found in the Supplementary Figures (S1) along with specific locations of the images.

[One to one point five column image, black and white]

A — 100 m
B — 50 m
C — 100 m
D — 50 m
E — 100 m
F — 100 m
G — 100 m
H — 50 m
I — 20 m
J — 50 m
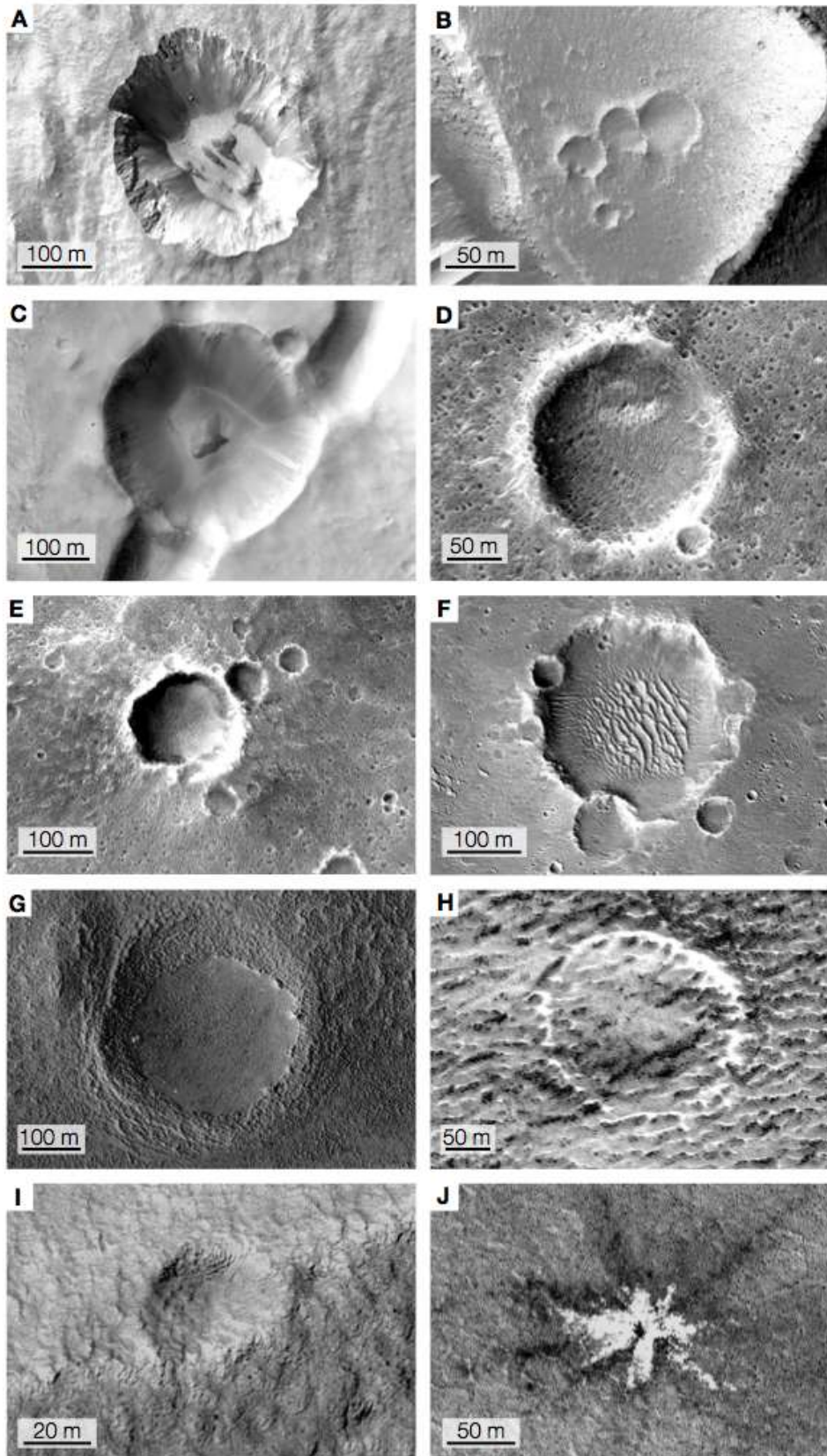
Figure 7 [crater morphology]. Examples of crater morphology and abundance, which can be used to gain an insight into the fundamental structure and composition of a terrain. Two examples are each given from Candor (including Central, Major East, Minor East, and Nia; A and B), Chryse (including Aram, Aureum, Hydaspis, and the Xanthe Terra crater; C and D), the highlands surrounding the chaos terrain (E and F), the Polar Layered Deposits (G and H), and the massive ice scarps identified by Dundas et al. (2018; I and J). A) A crater in Central Candor. B) A crater in Major East Candor Chaos. C) A crater in Aram Chaos. D) A crater in Aureum Chaos. E) A crater in the highlands near Aureum Chaos. F) A crater cluster in the highlands near Ganges Chasma. G) A young crater in the PLD gradually being infilled by ice by flexure of the substrate and annual ice deposition. H) An almost entirely infilled crater in the PLD. I) A possible crater associated with the massive ice scarps; craters were very difficult to find across multiple images, most likely due to their rapid loss by flexure of the ice substrate. J) A polar crater seasonally revisited by Dundas et al. (2014) over several Mars years to observe the repeated fluctuations of ice over time, potentially atop another ice-rich region. All image ID numbers can be found in the Supplementary Figures (S1) along with specific locations of the images.

[One to one point five column image, black and white]
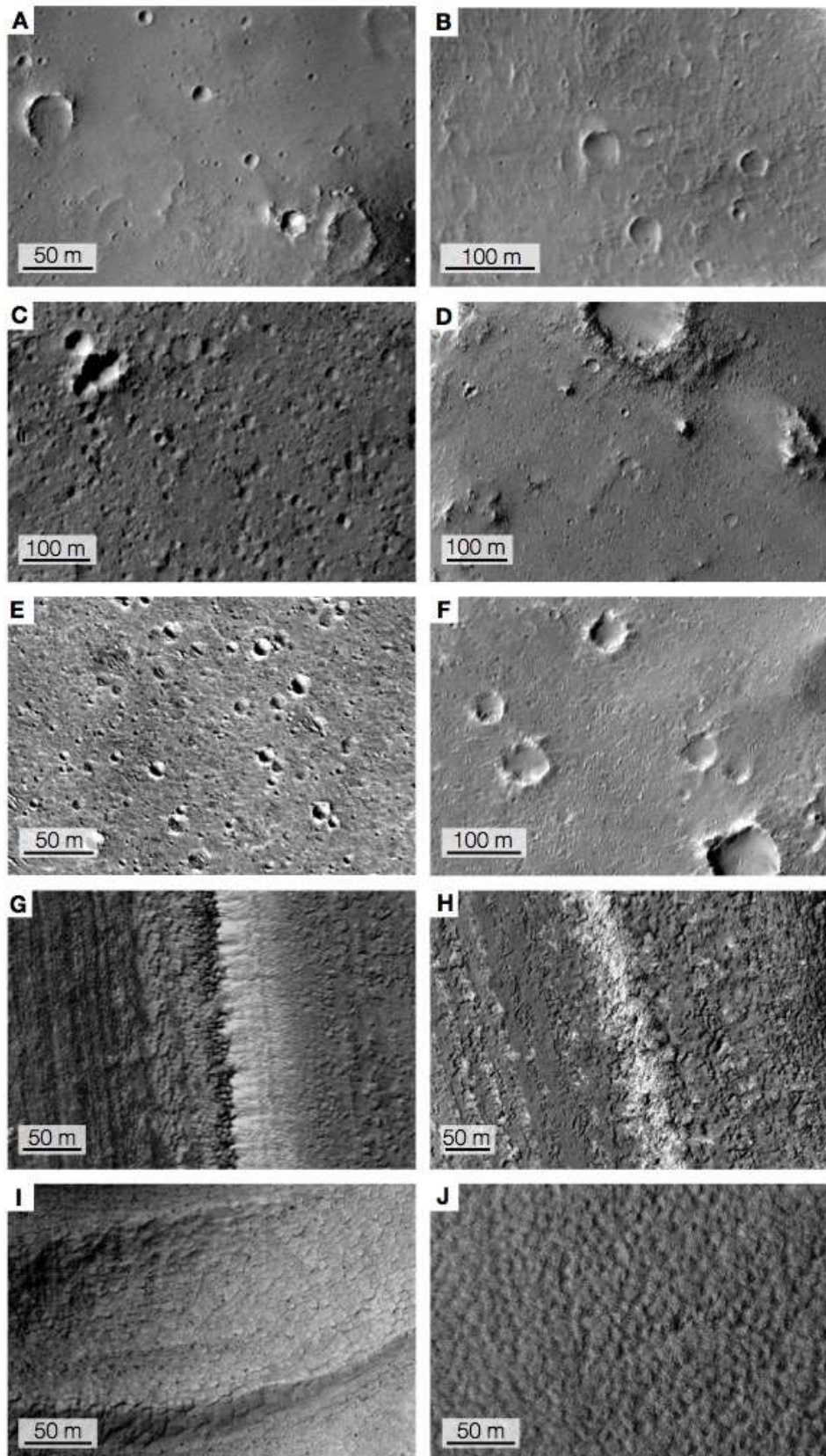
Figure 8 [terrain morphology]. Examples of crater morphology and abundance, which can be used to gain an insight into the fundamental structure and composition of a terrain. Two examples are each given from Candor (including Central, Major East, Minor East, and Nia; A and B), Chryse (including Aram, Aureum, Hydaspis, and the Xanthe Terra crater; C and D), the highlands surrounding the chaos terrain (E and F), the Polar Layered Deposits (G and H), and the massive ice scarps identified by Dundas et al. (2018; I and J). A) Cratered terrain in Nia Chaos, East Candor. B) Cratered terrain in Major East Candor Chaos. C) Crater-saturated terrain atop a mesa in Aureum Chaos. D) Terrain adjacent to Aureum Chaos. E) Crater-saturated terrain in the highlands north of Ganges Chasma. F) Cratered highlands south of Aureum Chaos. G) Typical terrain in the PLD, featuring dust and ice layers interbedded at varying scales. H) Another example of typical terrain in the PLD. I) General terrain in the regions adjacent to the Promethei Terra massive ice outcrops. Note the polygonal, smooth, uncratered texture, characteristic of an ice-rich substrate. J) A close-up of the polygonal texture that comprises the sites adjacent to the massive ice outcrops of Dundas et al. (2018). All image ID numbers can be found in the Supplementary Figures (S1) along with specific locations of the images.

[One to one point five column image, black and white.]

In *Fig. 6*, we compare the morphology of the boulders of Candor and Chryse to known sites of rock — highland terrain adjacent to Chryse — and massive ice — the north polar layered deposits (PLD) and the recently observed southern highland scarps described by Dundas et al. (2018). In *Fig. 7*, we compare typical craters found nearby such boulders for insight into the rheology of the subsurface: ice, for example, is known to viscously relax and may infill craters within on a timeline of centuries (Landis et al., 2016) and thus craters in such terrain will appear different to those in a rocky substrate. Lastly in *Fig. 8*, we image the wider terrain surrounding the boulder sites for more general characteristics such as cratering and texture. These criteria of boulders, craters, and terrain build distinct profiles for rock- or ice-dominated landscapes, granting us means of better understanding the composition of the fractured terrain in Candor and Chryse.

5.1.1. Boulders

Of the two examples of boulders at each type site (*Fig. 6*), those of Candor, Chryse, and the highlands (*Fig. 6a*, *b*, *c*, *d*, *e*, and *f*) appear very similar: they are usually dark, angular, roughly spherical, and associated with cliffs often lined with strata. Examples of boulders associated with the PLD (marked with arrows in *Fig. 6g* and *h*) are extremely scarce: though also found by strata-rich scarps, the two examples are tentative at best and may well be debris or ice protruding from the PLD. This is very unlike the situation in Candor, Chryse, and the highlands, where boulders are almost ubiquitous along slopes, especially when chaotically fractured. Herkenhoff et al. (2007) do describe boulders in PLD, but these are associated with dust- and sand-rich layers interbedded with the ice-rich layers that comprise the PLD. Boulders at sites of massive ice as described by Dundas et al. (2018; *Fig. 6i* and *j*) are similarly rare: those pictured are uncommon instances of rocky lenses entrained in the ice from which sediment is calving. They were not observed to change in position or morphology over three Martian years and were interpreted as rock for this reason, along with their association with the reddish-hued lens (Dundas et al., 2018). Elsewhere, boulders are not present. Exposed ice sublimates extremely quickly on Mars (Smith et al., 2009) and is not stable at the equator (Fanale et al., 1986; Baker, 2001), and while theoretical calculations and field observations show even extremely-thin debris layers may significantly inhibit rates of ice sublimation (Marchant et al., 2002; Kowalewski et al., 2006, 2011), the lack of boulders at ice-rich scarps implies either a sublimation rate higher than dust or debris accumulation rate, or a disinclination of the ice to calve. The rarity of boulders at sites of massive ice, and their abundance in rocky highland terrain, suggests the similar abundance of boulders in Candor and Chryse are more alike to those of the highlands'

rocky scarps.

5.1.2. Craters

The morphology of simple craters (less than 7 km diameter) varies within all sites, but two examples most representative of the standard are shown in *Fig. 7*. Again with PLD and the massive ice of Dundas et al. (2018), craters were scarce, which is unsurprising given their short viscous relaxation rates and their youthful age, and those present were either partially infilled (*Fig. 7g* and *h*), ambiguous (*Fig. 7i*), or they demonstrably unveiled ice that disappears and reappears seasonally (*Fig. 7j*, taken from Dundas et al., 2013). In contrast, craters in Candor, Chryse, and the highlands show high crater density in the terrain (*Fig. 7b*, *d*, *e*, and *f*) and have highly angular side profiles (*Fig. 7a* and *d*). Both of these characteristics suggest a rocky substrate, as craters in ice are lost over a matter of centuries (Landis et al., 2016) and pristine edges quickly soften with the downward slumping and infill associated with the viscous flow rates of an ice substrate, producing low depth-diameter ratios. Thus, cratering in Candor suggests the composition of the fractured blocks is structurally more similar to rock than to ice.

5.1.3. Terrain

The terrain of Candor, Chryse, and the highlands are dominated by high crater density in the range of 10-100 m craters (*Fig. 8a*, *b*, *c*, *d*, *e*, and *f*). In contrast, the terrain of the PLD is overwhelmingly dominated by its smoothed, characteristic layers of ice and dust (*Fig. 8g* and *h*) and the ice of Dundas et al. (2018; *Fig. 8i* and *j*) by smooth, polygonal fracturing. Both show a general absence of large craters implying a relatively young surface age, poor crater retention ability, and a fast rate of resurfacing. In contrast, the terrain of Candor, Chryse, and the highlands

represent the pristine record of intense impact gardening in the earlier periods of Martian history. This represents billions of years (see Hartmann and Neukum, 2001) rather than the estimated centuries (Landis et al., 2016) of cratering represented in icy terrain. The terrain of the fractured mesas in Candor thus shares more characteristics with landscapes composed of rock, not ice.

5.1.4. Summary of HiRISE study

The morphology of boulders, craters, and the general terrain of chaotic terrain in Candor appear far more alike to the rock-dominated landscape of the highlands and the Chryse Planitia than to ice-dominated landscapes. This is consistent with known deposits of modern ice on Mars, which are either latitude-dependent (~>30 °, e.g., Head and Marchant, 2003; Head et al., 2005; Hubbard et al., 2011; Dundas et al., 2013, 2018; Hubbard et al., 2014; Head and Weiss, 2014) or altitude-dependent (~>1.5 km above datum, e.g., Head et al., 2003; Shean et al., 2005, 2007; Fastook et al., 2008).
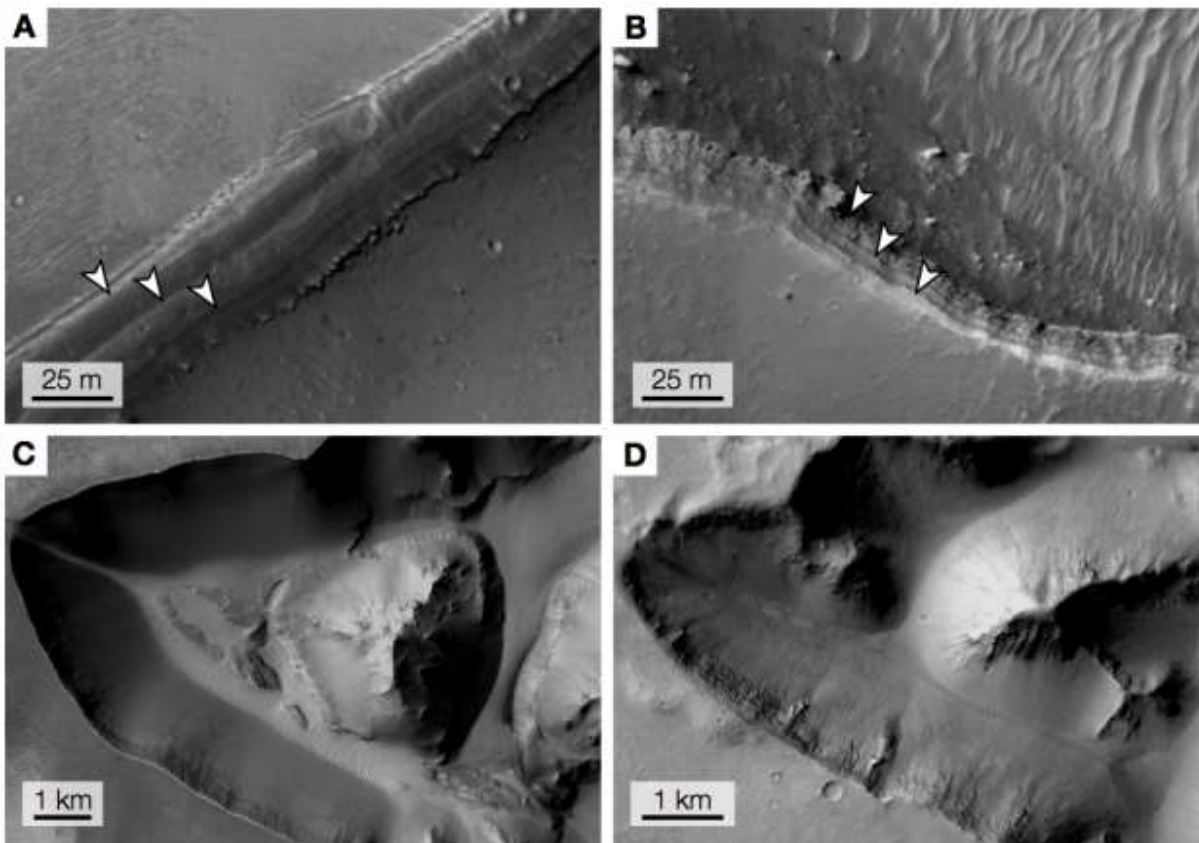
5.2. The 'outwash plains'

Glacial outwash plains — low-lying flat regions formed of glacial sediments deposited by meltwater outwash at the terminus of a glacier — were reported by Dębniak et al. (2017) in their regional map of Ius Chasma. Outwash plains on Earth (also called sandurs) are typically silt-, sand-, and boulder-rich, with material often size-sorted with silt and other fines deposited farthest from the source. Diffuse, braided streams commonly rework the deposits subsequent to deposition, and kettle holes may develop where stranded ice rafts disintegrate.

None of these characteristics are present in the mapped Ius deposit. Instead, the hummocky mounds appear massive in nature, alluring perhaps to an aeolian origin or from slumping with

chasma formation, with distinct and apparently unrelated fractured terrain underlying the unit.

Fig. 9 compares the morphology of the Ius features (*Fig. 9a* and *c*) with features of comparable morphology in Candor (*b*) and Chryse (*d*). In *Fig. 9a*, the edge of an Ius block is reminiscent of the edge of the chaotic blocks in Nia Chaos at identical scales, shown in *Fig. 9b*: visible strata are revealed intact (marked with arrows), boulders tumble down steep slopes, and the block surfaces themselves appear neither tilted nor affected by erosion or lateral movement. In *Fig. 9c* is an amphitheatre-shaped headland notch within the outwash plain, with a conical mound beside it. This is reminiscent of similarly back-wasted headlands in Aureum (*Fig. 9d*) at a similar scale, where conical mounds also form the same smoothed sides. Undisturbed strata, again, are also visible in *Figs. 9c* and *9d*.

The analysis of the Ius Chasma outwash plain in HiRISE does not reveal the smoothed, size-sorted, fluvial environment expected of an outwash plain (e.g., Gomez et al., 2000). Rather, the intact and pristine strata, the large boulders neither moved nor eroded from their parent slopes, and the clear distinction between blocks all bear more resemblance to chaotic terrain that has been partly covered by massive aeolian or slump material. The notched headland in *Fig. 9c* in particular is diagnostic of ground backwasting with the sapping of groundwater, and is a feature well-developed both in regions of violent groundwater expulsion such as the Chryse Planitia (*Fig. 9d*, in Aureum) and effusive such as the Louros and Nirgal Valles on the adjacent Thaumasia Plateau. Given the feature's symmetry and linearity it may have once been a pit chain, which are common across Marineris. These

Figure 9 [outwash plains]. A) HiRISE analysis of the 'outwash plain' of Dębniak et al. (2017), rather than displaying the rubbly, hummocky debris expected of an amorphous outwash plain, shows the edges of these blocks to display intact strata, marked by arrows. This bears significant morphological resemblance to the edges of angular Nia Chaos in East Candor (B). C) An amphitheater-shaped headland notch in the 'outwash plain' and a conical mound, both reminiscent of the groundwater sapping features in Central Candor Chasma (D). Morphology found in HiRISE images ESP_025561_1740_RED (A), PSP_009407_1730_RED (B), CTX images D02_027816_1728_XN_07S092W (C), and B18_016686_1738_XI_06S072W (D).

*[One column image, black and white.]*

observations are inconsistent with the glacial hypothesis, and the blocky terrain in Ius Chasma is interpreted here as another instance of chaos terrain within Marineris.

5.3. The 'trimline'

The 'trimline', revealed in HiRISE, appears less of a distinct morphological boundary and more a varying sequence of prominent strata, as exemplified with four individual outcrops in *Fig. 10*. In Ius Chasma (*Fig. 10a*), at least two distinct boundaries can be seen along the chasma wall. Furthermore in *Fig. 10b*, in Coprates Chasma, multiple units span the boundary and display varying profiles, which is inconsistent with both purportedly glacially-smoothed escarpments and the notion of a maximum level of glacial fill eroding all features below.

Fig. 10c further undermines this image of sub-boundary scoured walls: arrows denote multiple outcrops in Coprates where prominent bedrock remains regardless of its relative position to the boundary. *Fig. 10d* captures an observation that precludes a glacial trimline: a small landslide in Coprates Chasma, marked with arrows, has removed the wall's surface mantle only to reveal fresh, unweathered strata continuing beneath. A glacial trimline is a shallow, surficial feature that is easily removed by subsequent weathering or erosion, but here in Coprates the boundary continues horizontally along its strike.

We therefore conclude that this feature is not a trimline but is rather bedrock in the walls of Marineris itself. This is consistent with its observed continuousness, the multiple strata visible and their differing weathering profiles, and its variations in elevation, the latter which would be anticipated in the case that Marineris formed within ancestral basins (Schultz, 1998) or if sediment was deposited continuously during chasmata formation. These observations are therefore inconsistent with the glacial hypothesis.
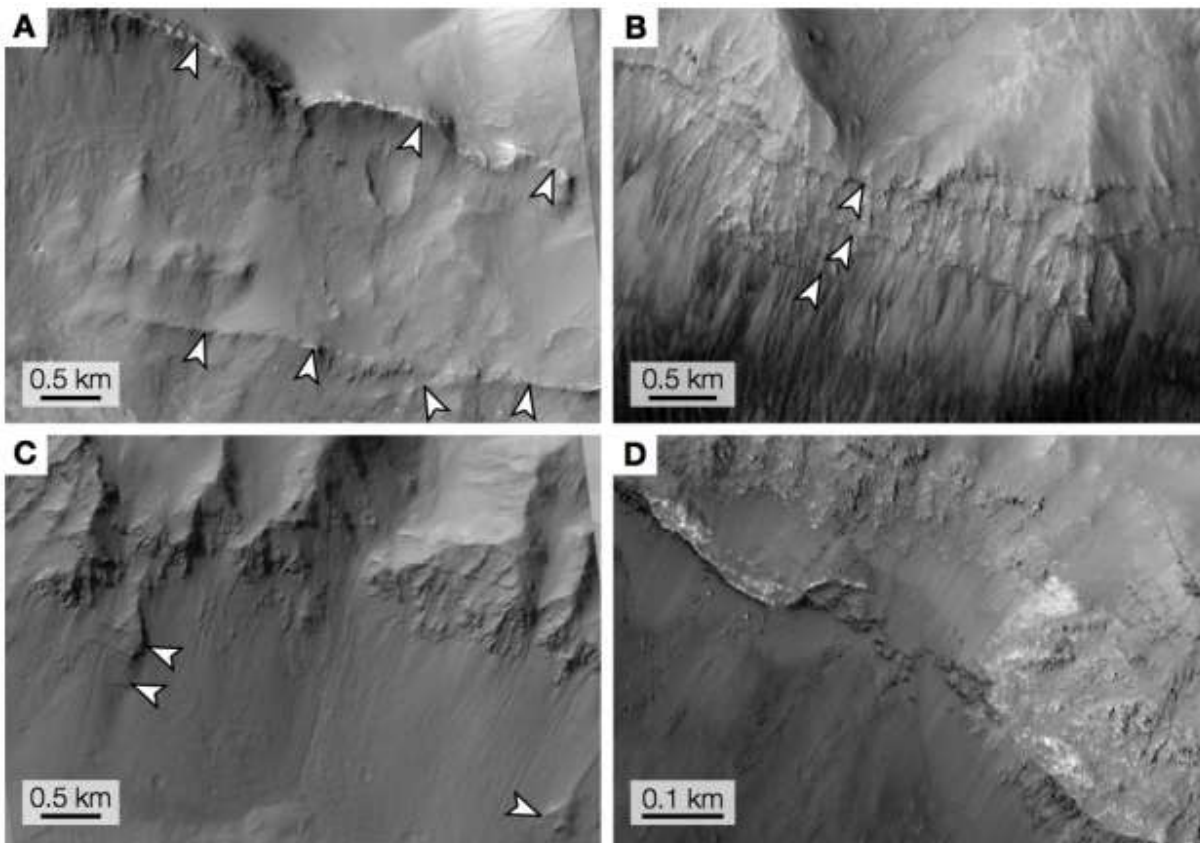
Figure 10 [trimline]. A) At least two morphological boundaries in Ius Chasma around the elevation of the supposed trimline, denoted by arrows. The uppermost boundary is at -4,107 m below the planetary datum, the lower at -4,122 m (MOLA data). B) Multiple distinct strata, examples marked with arrows, cut above and below the supposed trimline in Coprates Chasma. Between the topmost arrow and the bottommost is an elevation difference of 10.1 m (MOLA data). Were this a boundary denoting extreme erosion below, such intricate weathering profiles would have been eroded away. C) More prominent notches and strata below the boundary in Coprates Chasma, marked with arrows. D) A landslide in Coprates reveals the 'trimline' at -3,193 m to continue beneath the scar as part of a strata that continues from one side of the image to the other. Dark patch is the landslide; the bright material appears to be the weathered surface of the chasma wall, which was removed where the landslide occurred. Morphology found in HiRISE images ESP_046000_1730 (A), ESP_013587_1685 (B), ESP_025705_1675 (C), and ESP_047779_1655 (D).

[One column image, black and white].

5.4. Slope profile analysis

For some quantification of the difference between icy and rocky substrates, we extracted topographic data from the Mars Orbital Laser Altimeter (MOLA; on the order of 463 m^{-1}/pixel) to quantify the slope profiles of these blocks in the Candor and Chryse regions for comparison with each other, and then with the ice- and dust-rich slopes of the PLD. Two chaos blocks (or in the case of the PLD, slopes at two different sites) were selected for study from each site — Central Candor, Aram, Aureum, Hydaspis, Xanthe Terra crater, and the PLD — and through these four profiles were taken to compile a three-dimensional picture of the feature from multiple angles. Chaos blocks were selected for analysis based on the following criteria: they had to be sufficiently large (>2 km) to be resolved by MOLA resolution, and ideally they were free-standing (i.e., not connected to other mesas through shallow cracks) and not abutting dunes or other unrelated material that would affect the profile. For the PLD slopes, as there are no mesas in this region and we were interested more in the curvature of a slope's profile over similar distances, four adjacent slopes within the same CTX image were selected to best understand the general profile of an ice-rich terrain. No data was extracted from the massive ice slopes of Dundas et al. (2018) as the scarps fell below the resolution of MOLA data. The results are displayed in *Fig. 11*, and all additional data, including data points for all profiles, their CTX image IDs, their locations, can be found in the Supplementary Figures (S2). The transects run either from left to right or top to bottom, and colours denote no meaning beyond distinguishing one transect from another.
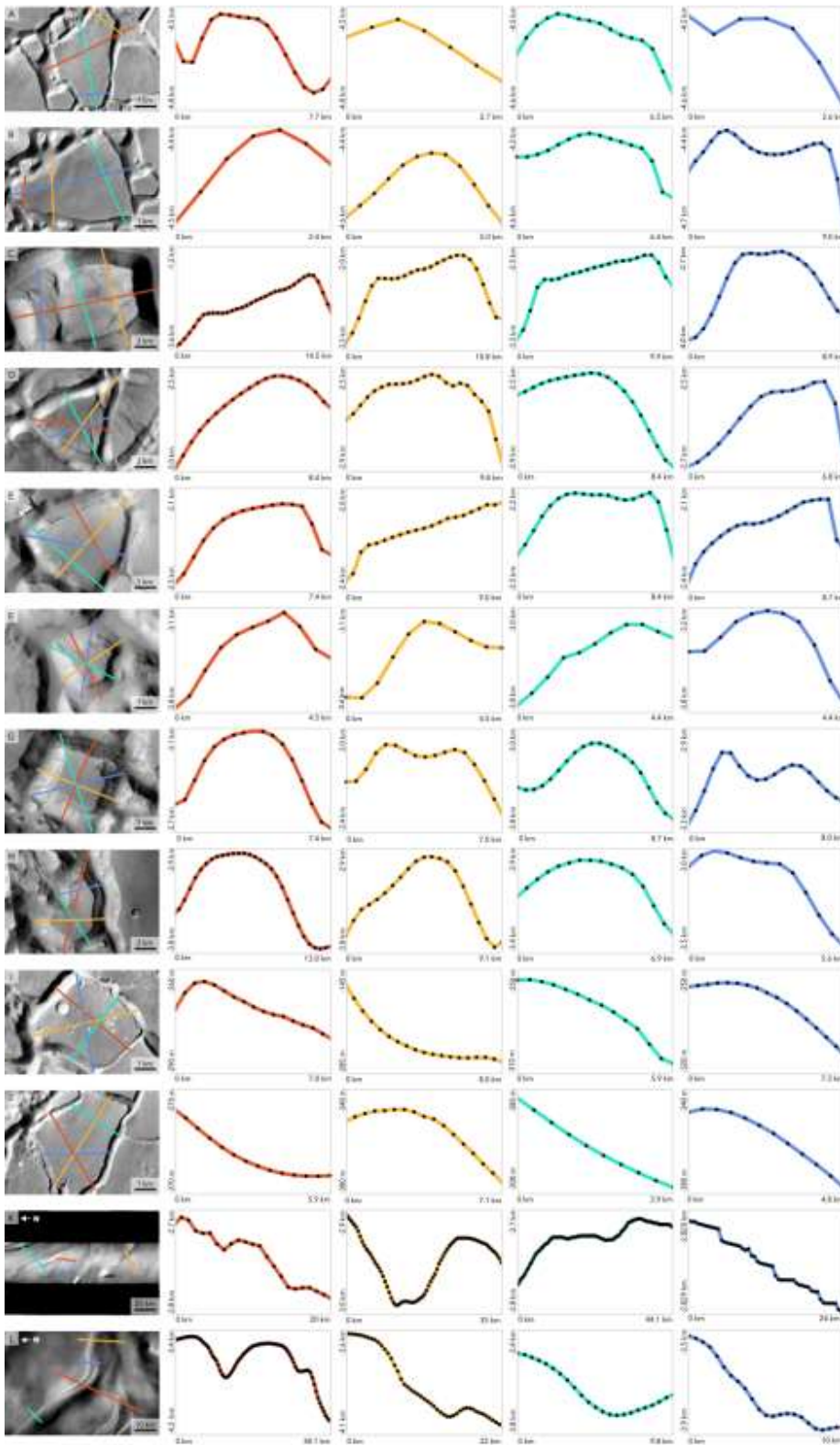
Figure 11 [slope profiles]. Slope profiles taken through individual mesas in Candor and Chryse, and along adjacent slopes in the polar layered deposits. This is to gauge a sense of their three-dimensional shapes and whether the chaos in Candor bears more similarity in slope shape to the known ice composition of the PLD or the known rock composition of the Chryse chaos. Colours do not hold meaning beyond distinguishing individual transects. Lines are straight between individual MOLA data points, which are marked by black circles. A) Four sections through a mesa in Candor Chaos. B) Four sections through an additional mesa in Candor Chaos. C) Four sections through a mesa in Aram Chaos. D) Four sections through an additional mesa in Aram Chaos. E) Four sections through a mesa in Aureum Chaos. F) Four sections through an additional mesa in Aureum Chaos. G) Four sections through a mesa in Hydaspis Chaos. H) Four sections through an additional mesa in Hydaspis Chaos. I) Four sections through a mesa in the fractured unnamed crater in Xanthe Terra. J) Four sections through an additional mesa in the fractured unnamed crater in Xanthe Terra. K) Four sections across a central part of the north polar ice cap. L) Four sections across a scarp near the periphery of the north polar ice cap, with the PLD clearly visible. All image IDs and locations found in Supplementary Figures (S2).

[two column image, black and white cannot be used.]

While the extent of rounding in these profiles is likely an artefact of the interpolation of MOLA shot points, the profiles reveal that the tops of chaos mesas in Candor and Chryse are not as flat as they appear aerially. This is perhaps unsurprising given their origins from the gently-sloping surrounding highland terrain. The blocks tend to have distinctive, steep-walled slopes: *Fig. 11a* (Candor), *11c* (Aram), and *11g* (Hydaspis) are exceptional examples of how sharply these mesas rise above the basin floor. Chaos raft height is mostly on the order of several hundred metres, though there are some instances of a kilometre or more (e.g., *Fig. 11c*).

There appears to be little difference between the Candor and Chryse examples; indeed, the main source of difference within the chaos terrains is the Xanthe Terra crater from the rest. This fractured crater is set near the planetary datum in the highlands away from the scoured basins where Aram, Aureum, and Hydaspis lie, its chaos rafts more shallowly fractured and

interconnected. As previously noted, chaos terrain development in the Xanthe Terra crater is significantly less developed than our other Chryse examples, exhibiting no outflow channels or even rounded chaos blocks, implying fluid expulsion was minimal and perhaps as one minor event. The slope profiles of *Figs. 11i* and *j* demonstrate this: unlike the distinctive steep walled and relatively flat-topped profiles of *Figs. 11a-h*, the profiles of the Xanthe Terra crater better reflect this inward collapse. *Fig. 11i* is from a block located along the western edge of the crater (specific locations in the Supplementary Figures, S2) and dips east and southeast to the centre of the crater; likewise *Fig. 11j* is from the crater's northwest edge and it dips centrally to the south and southeast.

Though difficult to make direct comparisons of the slopes of Candor and Chryse with the PLD as no similar blocky terrain is found at the poles, in *Figs. 11k* and *11l* are two examples of this terrain with four profiles likewise drawn. *Fig. 11k* is located far north in the central rise of the north polar ice cap, while *Fig. 11l* is a scarp from the periphery of the ice cap with the PLD clearly visible. A step-like morphology occurs in both, particularly in the third and fourth transects of *Fig. 11k*, ad this is a feature not observed in Candor and Chryse.

Relating to the reasoning of Gourronc et al. (2014) that the chaotic terrain in Candor is ice, these profiles do not suggest any fundamental difference in substrate between the blocks of Candor and Chryse; rather, as the Xanthe Terra crater shows, slope profiles of the blocky terrain show more dissimilarity *within* Chryse than in comparison with Candor, and are perhaps dependent upon the magnitude of the fracturing event.

5.5. The lateral moraines

Lastly, we discuss the lateral moraines that were described in Ius and Capri Chasmata by

Gourronc et al. (2014), interchangeably therein referred to as lateral moraines/banks/benches. Lateral moraines are moraines occupying the lateral margins of glaciers that lie within valleys, but upon closer analysis we were unable to find in Ius Chasma any feature remotely akin to these hummocky, poorly-consolidated, steeply-angled mounds. In Capri Chasma, the images used by Gourronc et al. (2014) as examples of lateral moraines appear
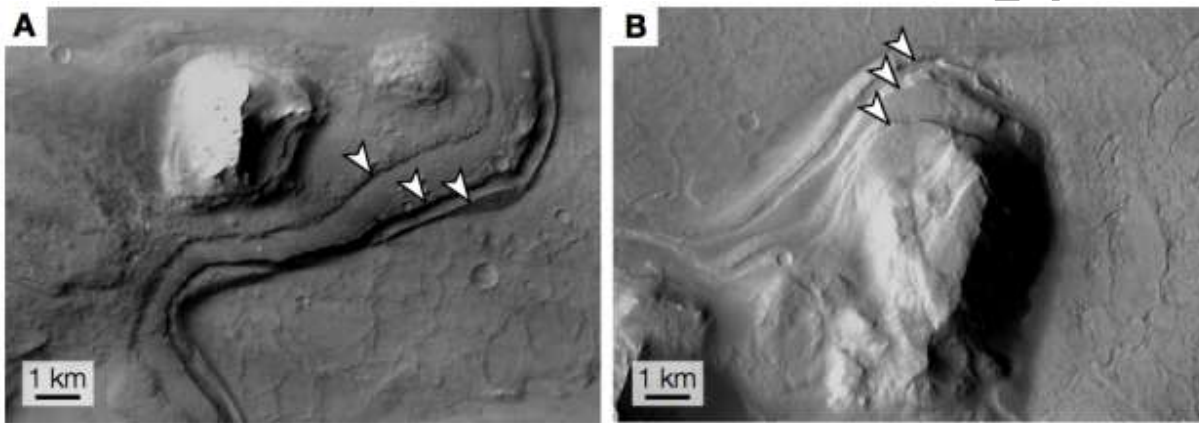
Figure 12 [lateral moraines]. Two examples of possible lateral moraines (Gourronc et al., 2014) or lake terraces (Harrison and Chapman, 2008) both in Coprates Chasma. These do not resemble in any way the morphology of lateral moraines found on Earth. A) B17_016303_1649_XN_15S053W. B) F06_038179_1651_XN_14S052W. (Both CTX images).

[one column image, black and white.]

more platform-like, clearly emerging seamlessly from chasma walls (two examples given in *Fig. 12*). These may be a continuation of the strata themselves given the platforms' close alignment with strata in the chasma walls: high-definition geomorphologic analysis in this region has previously revealed a stratigraphy comprising alternating thin, strong layers and thicker, relatively weak layers (Beyer and McEwen, 2005), which could account for one protruding while another is eroded away. Alternatively, the features have previously been interpreted as lake shorelines (Harrison and Chapman, 2008).

It is worth considering that the lifetime of lateral moraines on Earth is extremely short. This is because, given their by-definition loosely-consolidated and often ice-cored nature, they undergo rapid post-glacial collapse: Hambrey (2004) notes a discerning eye is required to identify even a 10 Kyr old example on Earth. The survival of such a feature for ~3 Gyr on Mars is therefore exceedingly improbable even with expected Martian erosion rates at two to five orders of magnitude slower than on Earth (Golombek et al., 2006, 2014; Sweeney et al., 2018). Lateral moraines commonly waste by gravity-driven sedimentary flow into tessellated fans (Bennett et al., 2000), or by collapse and reworking following removal of buttressing ice (Curry et al., 2009), but neither glacio-fluvial nor collapse features can be seen in association with the structures in *Fig. 12* . Even supposing such structures' integrity was maintained by Mars' sub-zero surface temperatures, these bench-like platforms of within Coprates and Capri Chasmata bear no resemblance to the piles of loose material that are glacial moraines of any sort.

6. DISCUSSION

Our morphological study of Candor Chaos and blocky terrain in East Candor and Ius has revealed their morphological indistinguishability from the circum-Chryse chaos terrain. Therefore, if Candor's chaos is to be reinterpreted as fractured ice, as per the suggestion of Gourronc et al. (2014), so too must all chaos terrain on Mars. A conclusion better supported by evidence is that terrain in Central Candor, East Candor, and Ius instead follows the more common interpretation of chaos as a collapse feature following the expulsion of some subsurface fluid. Two implications of this conclusion are now discussed.

6.1. Implication I: The lack of a Marineris glacier

We demonstrate in our literature review in Section 2 that features given as structural and mineralogical evidence in support of the glacial Marineris hypothesis find more plausible origins in tectonic reorganisation and groundwater sapping. We also demonstrate, both in Section 2 and in our in-depth morphological results in Section 4 and its discussion in Section 5, that morphological evidence in support of the glacial Marineris hypothesis find more plausible origins through the expulsion of groundwater. Thus, we find no evidence in support of the glacial Marineris hypothesis.

This conclusion is consistent with a growing view of the Late Noachian-Late Hesperian Martian climate as one cold and dry with limited precipitation (Fastook and Head, 2015; Wordsworth et al., 2015; Carr and Head, 2015; Wordsworth et al., 2017), where ice accumulates in the southern highlands and draws water away from the northern lowlands. Climate would be less relevant with a groundwater source for the glacier; however, while Mars' total inventory of water is continually debated and amended (e.g., Lunine et al., 2003; Clifford et al., 2010; Kurokawa et al., 2014; Levy et al., 2014; Carr and Head, 2015; Villanueva et al., 2015; Clifford and McCubbin, 2016; Haberle et al., 2017) and it is plausible that deep reserves remain buried beyond the scope of surface-based probes, the sheer volume of the Marineris glacier is comparable with that of the Oceanus Borealis hypothesis for an ocean covering up to a third of the Martian surface (e.g., Baker, 2001; Clifford and Parker, 2001). This idea has been strongly criticised for its incompatibility with current understanding of the Martian global water budget and timing: from once considering as much as $\sim 2.3 \times 10^7$ km^3 of flood waters from the Chryse Planitia inundating the northern lowlands at once (Carr and Head, 2003), episodic events of lower magnitude over a longer period of time now appear far more probable (Warner et al., 2010, 2011; Rodríguez et al., 2015). This removes the need for high volumes of liquid water

existing at once in any one period of Martian history. The volume given for the Marineris glaciation is very loosely defined, lacking both vertical and horizontal constraints, and is given on the order of 10^6 km^3 (Gourronc et al., 2014) — a significant proportion of the total circum-Chryse outflow channels' volume, and on par with the Martian north and south polar ice caps' $(1.2 \times 10^6\text{-}1.7 \times 10^6$ km^3 and $2 \times 10^6\text{-}3 \times 10^6$ km^3, respectively; Smith et al., 1999). Such a vast body of water existing at this point in the planet's history disagrees with an evolving understanding of a water-limited Martian surface.

Our conclusion is also consistent with present understanding of Martian obliquity cycles. Mars' obliquity is presently at 25.9°, but obliquity may have reached up to 46° within the last 10 Ma alone (Laskar et al., 2002, 2004) forcing the fall of equatorial ground temperatures while poles experience warming. Gourronc et al. (2014) invoke this extreme obliquity-driven precipitation to account for at least 3 km^3 of climate-driven snowfall in Marineris, yet acknowledge the absence of re-glaciations based on the pristineness of intra-chasma landslides aged 3.5 Ga and younger (Quantin et al., 2004a, 2004b). Were glaciation obliquity-driven, repeated and distinct episodes of such massive ice accumulation would be expected in Marineris and are not found. The uniqueness of the Marineris episode would suggest a non-obliquity related mechanism, but no singular climatic event has been proposed to account for such a vast fill.

Finally, a glacial fill cannot be reconciled with the absence of either the remains of a basin wall or some tangible evidence of proglacial margins or plains. The terminus of a glacier is a complex environment characterised by high energy outwash plains and/or deflation moraine such as hummocks, kames and kettle holes, and push or terminal moraine that can cover many thousands of kilometres. Such features have not been identified at the outlet of Marineris where

Coprates Chasma meets Capri Chasma and opens to the Chryse Planitia. Alternatively, the glacier could have been confined within a basin prior to the opening of the chasmata's eastern end: a wall between Coprates and Capri Chasmata has been proposed where the two narrow to 15 km across, collapse of which may have occurred by backwasting of Eos Chaos (Flahaut et al., 2010), tectonism with ongoing chasmata formation (Dohm et al., 2001), downward erosion by overtopping water (Harrison and Chapman, 2010), and/or surface collapse by dissolution of chasma wall (Rodríguez et al., 2003). Regardless of the timing of both the proposed glacier and the wall's loss, which are ambiguous, only two scenarios exist: either the glacier existed prior to the wall's loss in an enclosed basin, or subsequently in an open valley. In both cases, such delicate glacial features cited by Gourronc et al. (2014) would be destroyed either through continued chasmata formation or the downgradient flow of ice, which even under extremely low slope gradient and temperatures has the capacity for movement on Earth (Cuffey et al., 2000; Waller, 2001; Atkins et al., 2002; Head and Marchant, 2003). No features indicative of such flow exist in Coprates or Capri Chasmata where flow would be expected to be most concentrated, whether subglacially such as flutings, eskers, crevasse-squeeze ridges, traction till, or a *u*-shaped chasma profile (see overview by Benn and Evans, 2014; Evans et al., 2006; Dowdeswell et al., 2010), or proglacially such as kame and kettle holes, pitted sandur plains, or push, latero-frontal, hummocky, and terminal moraine, (see overview by Benn and Evans, 2014; Hambrey et al., 1997; Evans and Twigg, 2002). Thus, the reported pristineness of the relict glacier cannot be reconciled with either the tectonic history of Marineris or the absence of flow geomorphology.

Thus we reach the main conclusion of this research: we find no evidence to support the existence of a glacier, erstwhile or extant, in Valles Marineris.

6.2. Implication II: The presence of groundwater in Marineris

Chaos terrain, as has been established, forms by the pressurisation and expulsion of a subsurface fluid, and as we have here established, the chaotic terrain of Candor and Ius formed no differently. This requires that Marineris, like Chryse, was affected too by the regional aquifer and its violent eruption to the surface. Groundwater therefore flowed and pooled in Candor and Ius Chasma from the late Hesperian to early Amazonian when such outflow events commonly occurred (e.g., Ivanov and Head, 2001; Warner et al., 2009, 2010, 2011, 2013; Rodríguez et al., 2011, 2015), and was a source of at least transiently liquid water in the chasmata's interior. Lacustrine and fluvial activity have been proposed across the chasmata system (Mangold et al., 2006; Quantin et al., 2005; Di Achille et al., 2006; Weitz et al., 2006; Harrison and Chapman, 2008, 2010; Metz et al., 2009; Flahaut et al., 2010; Warner et al., 2013), with groundwater frequently cited as their source. Hence, a groundwater origin for the chaos in interior Marineris is consistent with the regional hydrology.

The presence of groundwater in interior Marineris is not surprising given the long-known association of groundwater pooling within deep localities, as recently quantified in Gale Crater where understanding of a lake both groundwater and precipitation-fed is slowly crystallising (Hurowitz et al., 2017). Additionally, Marineris is the deepest point for a radius of a thousand kilometres and lakes here in such deep regions have been previously hypothesised as groundwater-fed (e.g., Warner et al., 2013). On a broader scale, evidence of groundwater in the form of chaos and notched headland valles occurs at every point of weakness immediately at the valles of Echus, Juventae, Hebes, and Ganges, immediately east of Marineris in Capri Chaos, and further east to the chaos of the neighboring Chryse Planitia.

It appears that Marineris and the connecting Chryse Planitia are two regions on Mars where

the geologic history has been dominated and defined by the activity of groundwater. From this second implication of our research we consider a possibility: that groundwater in Valles Marineris could have permitted late-stage lacustrine and/or other forms of aqueous activity in this area independently of climate.

7. CONCLUSIONS

The reaffirmation of chaos terrain as fractured rock in interior Marineris is inconsistent with the ice disintegration continuum of Gourronc et al. (2014), the main line of evidence for the glaciated Marineris hypothesis. Furthermore, we find more reasonable explanations for other supposedly glacial characteristics — such as *sackungen* spreading ridges, perched regions of jarosite, outwash plains, kame and kettle holes, and trimlines — that do not require glaciation. While large deposits of ice hidden from visible-light cameras or shallow radar are infrequently discovered (e.g., Guidat et al., 2015; Stuurman et al., 2016; Dundas et al., 2018), a compelling morphological argument can be drawn against an ice-rich substrate for chaos terrain. We thus do not support the notion of a glaciation within the Valles Marineris, whether erstwhile or extant. Instead, we note that the presence of chaos in Candor Chasma points to an intriguing source of groundwater within the chasmata, which researchers of aqueous activity within Marineris may find of significant interest.

ACKNOWLEDGEMENTS

making public their Mars Orbiter Laser Altimeter data, and also the Mars Reconnaissance

Orbiter team for their continued release of Context Camera (NASA/JPL/Malin Space Science

Systems) and High Resolution Imaging Science Experiment (NASA/JPL/University of Arizona)

images.

DECLARATIONS OF INTEREST: None.

REFERENCES

Andrews-Hanna, J.C., 2012. The formation of Valles Marineris: 3. Trough formation through

super-isostasy, stress, sedimentation, and subsidence. J. Geophys. Res. Planets 117, E06002.

https://doi.org/10.1029/2012JE004059

Andrews-Hanna, J.C., Phillips, R.J., 2007. Hydrological modeling of outflow channels and chaos

regions on Mars. J. Geophys. Res. Planets 112, E08001. https://doi.org/10.1029/2006JE002881

Atkins, C.B., Barrett, P.J., Hicock, S.R., 2002. Cold glaciers erode and deposit: Evidence from

Allan Hills, Antarctica. Geology 30, 659–662. https://doi.org/10.1130/0091-

7613(2002)030<0659:CGEADE>2.0.CO;2

Baker, V.R., 2001. Water and the martian landscape [WWW Document]. Nature. URL

https://www.nature.com/articles/35084172 (accessed 4.30.18).

Ballantyne, C.K., 1997. Periglacial trimlines in the Scottish Highlands. Quat. Int. 38-39, 119–

136. https://doi.org/10.1016/S1040-6182(96)00016-X

Battler, M.M., Osinski, G.R., Lim, D.S.S., Davila, A.F., Michel, F.A., Craig, M.A., Izawa,

M.R.M., Leoni, L., Slater, G.F., Fairén, A.G., Preston, L.J., Banerjee, N.R., 2013.

Characterisation of the acidic cold seep emplaced jarositic Golden Deposit, NWT, Canada, as an

analogue for jarosite deposition on Mars. Icarus, Terrestrial Analogs for Mars: Mars Science Laboratory and Beyond 224, 382–398. https://doi.org/10.1016/j.icarus.2012.05.015

Benn, D., Evans, D.J., 2014. Glaciers and glaciation. Routledge.

Bennett, M.R., Huddart, D., Glasser, N.F., Hambrey, M.J., 2000. Resedimentation of debris on an ice-cored lateral moraine in the high-Arctic (Kongsvegen, Svalbard). Geomorphology 35, 21–40. https://doi.org/10.1016/S0169-555X(00)00017-9

Beyer, R.A., McEwen, A.S., 2005. Layering stratigraphy of eastern Coprates and northern Capri Chasmata, Mars. Icarus 179, 1–23. https://doi.org/10.1016/j.icarus.2005.06.014

Bovis, M.J., Evans, S.G., 1996. Extensive deformations of rock slopes in southern Coast Mountains, southwest British Columbia, Canada. Eng. Geol. 44, 163–182. https://doi.org/10.1016/S0013-7952(96)00068-3

Brož, P., Hauber, E., Wray, J.J., Michael, G., 2017. Amazonian volcanism inside Valles Marineris on Mars. Earth Planet. Sci. Lett. 473, 122–130. https://doi.org/10.1016/j.epsl.2017.06.003

Carr, M.H., 1979. Formation of Martian flood features by release of water from confined aquifers. J. Geophys. Res. Solid Earth 84, 2995–3007. https://doi.org/10.1029/JB084iB06p02995

Carr, M.H., Head, J.W., 2015. Martian surface/near-surface water inventory: Sources, sinks, and changes with time. Geophys. Res. Lett. 42, 2014GL062464. https://doi.org/10.1002/2014GL062464

Carr, M.H., Head, J.W., 2003. Oceans on Mars: An assessment of the observational evidence and possible fate. J. Geophys. Res. Planets 108.

Chapman, M.G., Soderblom, L.A., Cushing, G., 2005. Evidence of Very Young Glacial Processes in Central Candor Chasma, Mars. Presented at the 36th Annual Lunar and Planetary

Science Conference.

Chapman, M.G., Tanaka, K.L., 2002. Related Magma–Ice Interactions: Possible Origins of Chasmata, Chaos, and Surface Materials in Xanthe, Margaritifer, and Meridiani Terrae, Mars. Icarus 155, 324–339. https://doi.org/10.1006/icar.2001.6735

Clifford, S., Lasue Jeremie, Heggy Essam, Boisson Joséphine, McGovern Patrick, Max Michael D., 2010. Depth of the Martian cryosphere: Revised estimates and implications for the existence and detection of subpermafrost groundwater. J. Geophys. Res. Planets 115. https://doi.org/10.1029/2009JE003462

Clifford, S.M., McCubbin, F.M., 2016. How Well Does the Present Surface Inventory of Water on Mars Constrain the Past? Presented at the Lunar and Planetary Science Conference, 21-25 Mar. 2016, United States.

Clifford, S.M., Parker, T.J., 2001. The evolution of the Martian hydrosphere: Implications for the fate of a primordial ocean and the current state of the northern plains. Icarus 154, 40–79.

Cuffey, K.M., Conway, H., Gades, A.M., Hallet, B., Lorrain, R., Severinghaus, J.P., Steig, E.J., Vaughn, B., White, J.W.C., 2000. Entrainment at cold glacier beds. Geology 28, 351–354. https://doi.org/10.1130/0091-7613(2000)28<351:EACGB>2.0.CO;2

Cull, S., McGuire, P.C., Gross, C., Myers, J., Shmorhun, N., 2014. A new type of jarosite deposit on Mars: Evidence for past glaciation in Valles Marineris? Geology 42, 959–962. https://doi.org/10.1130/G36152.1

Curry, A.M., Sands, T.B., Porter, P.R., 2009. Geotechnical controls on a steep lateral moraine undergoing paraglacial slope adjustment. Geol. Soc. Lond. Spec. Publ. 320, 181–197. https://doi.org/10.1144/SP320.12

Dębniak, K., Mège, D., Gurgurewicz, J., 2017. Geomorphology of Ius Chasma, Valles Marineris,

Mars. J. Maps 13, 260–269. https://doi.org/10.1080/17445647.2017.1296790

Di Achille, G., Ori, G.G., Reiss, D., Hauber, E., Gwinner, K., Michael, G., Neukum, G., 2006. A steep fan at Coprates Catena, Valles Marineris, Mars, as seen by HRSC data. Geophys. Res. Lett. 33, L07204. https://doi.org/10.1029/2005GL025435

Discenza, M.E., Esposito, C., Martino, S., Petitta, M., Prestininzi, A., Mugnozza, G.S., 2011. The gravitational slope deformation of Mt. Rocchetta ridge (central Apennines, Italy): geological-evolutionary model and numerical analysis. Bull. Eng. Geol. Environ. 70, 559–575. https://doi.org/10.1007/s10064-010-0342-7

Dowdeswell, J.A., Hogan, K.A., Evans, J., Noormets, R., Cofaigh, C.Ó., Ottesen, D., 2010. Past ice-sheet flow east of Svalbard inferred from streamlined subglacial landforms. Geology 38, 163–166. https://doi.org/10.1130/G30621.1

Dramis, F., Sorriso-Valvo, M., 1995. Deep-seated gravitational slope deformations, related landslides and tectonics. Int. J. Rock Mech. Min. Sci. Geomech. Abstr. 5, 203A.

Dundas, C., Byrne Shane, McEwen Alfred S., Mellon Michael T., Kennedy Megan R., Daubar Ingrid J., Saper Lee, 2013. HiRISE observations of new impact craters exposing Martian ground ice. J. Geophys. Res. Planets 119, 109–127. https://doi.org/10.1002/2013JE004482

Dundas, C.M., Bramson, A.M., Ojha, L., Wray, J.J., Mellon, M.T., Byrne, S., McEwen, A.S., Putzig, N.E., Viola, D., Sutton, S., 2018. Exposed subsurface ice sheets in the Martian mid-latitudes. Science 359, 199–201.

Evans, D.J.A., Phillips, E.R., Hiemstra, J.F., Auton, C.A., 2006. Subglacial till: formation, sedimentary characteristics and classification. Earth-Sci. Rev. 78, 115–176.

Evans, D.J., Twigg, D.R., 2002. The active temperate glacial landsystem: a model based on Breiḥamerkurjökull and Fjallsjökull, Iceland. Quat. Sci. Rev. 21, 2143–2177.

Fanale, F.P., Salvail, J.R., Zent, A.P., Postawko, S.E., 1986. Global distribution and migration of subsurface ice on Mars. Icarus 67, 1–18.

Fastook, J.L., Head, J.W., 2015. Glaciation in the Late Noachian Icy Highlands: Ice accumulation, distribution, flow rates, basal melting, and top-down melting rates and patterns. Planet. Space Sci. 106, 82–98. https://doi.org/10.1016/j.pss.2014.11.028

Fastook, J.L., Head, J.W., Marchant, D.R., Forget, F., 2008. Tropical mountain glaciers on Mars: Altitude-dependence of ice accumulation, accumulation conditions, formation times, glacier dynamics, and implications for planetary spin-axis/orbital history. Icarus 198, 305–317.

Fueten, F., Flahaut, J., Le Deit, L., Stesky, R., Hauber, E., Gwinner, K., 2011. Interior layered deposits within a perched basin, southern Coprates Chasma, Mars: Evidence for their formation, alteration, and erosion. J. Geophys. Res. Planets 116, E02003. https://doi.org/10.1029/2010JE003695

Fueten, F., Flahaut, J., Stesky, R., Hauber, E., Rossi, A.P., 2014. Stratigraphy and mineralogy of Candor Mensa, West Candor Chasma, Mars: Insights into the geologic history of Valles Marineris. J. Geophys. Res. Planets 119, 2013JE004557. https://doi.org/10.1002/2013JE004557

Gendrin, A., Mangold, N., Bibring, J.-P., Langevin, Y., Gondet, B., Poulet, F., Bonello, G., Quantin, C., Mustard, J., Arvidson, R., LeMouélic, S., 2005. Sulfates in Martian Layered Terrains: The OMEGA/Mars Express View. Science 307, 1587–1591. https://doi.org/10.1126/science.1109087

Glotch, T.D., Christensen, P.R., 2005. Geologic and mineralogic mapping of Aram Chaos: Evidence for a water-rich history. J. Geophys. Res. Planets 110, E09006. https://doi.org/10.1029/2004JE002389

Glotch, T.D., Rogers, A.D., 2007. Evidence for aqueous deposition of hematite- and sulfate-rich

light-toned layered deposits in Aureum and Iani Chaos, Mars. J. Geophys. Res. Planets 112, E06001. https://doi.org/10.1029/2006JE002863

Golombek, M.P., Grant, J.A., Crumpler, L.S., Greeley, R., Arvidson, R.E., Bell, J.F., Weitz, C.M., Sullivan, R., Christensen, P.R., Soderblom, L.A., Squyres, S.W., 2006. Erosion rates at the Mars Exploration Rover landing sites and long-term climate change on Mars. J. Geophys. Res. Planets 111. https://doi.org/10.1029/2006JE002754

Golombek, M.P., Warner, N.H., Ganti, V., Lamb, M.P., Parker, T.J., Fergason, R.L., Sullivan, R., 2014. Small crater modification on Meridiani Planum and implications for erosion rates and climate change on Mars. J. Geophys. Res. Planets 119, 2522–2547. https://doi.org/10.1002/2014JE004658

Gomez, B., Smith, L.C., Magilligan, F.J., Mertes, L. a. K., Smith, N.D., 2000. Glacier outburst floods and outwash plain development: Skeiäarársandur, Iceland. Terra Nova 12, 126–131. https://doi.org/10.1046/j.1365-3121.2000.123277.x

Gourronc, M., Bourgeois, O., Mège, D., Pochat, S., Bultel, B., Massé, M., Le Deit, L., Le Mouélic, S., Mercier, D., 2014. One million cubic kilometres of fossil ice in Valles Marineris: Relics of a 3.5 Gy old glacial landsystem along the Martian equator. Geomorphology 204, 235–255. https://doi.org/10.1016/j.geomorph.2013.08.009

Grimm, R., Harrison Keith P., Stillman David E., Kirchoff Michelle R., 2017. On the secular retention of ground water and ice on Mars. J. Geophys. Res. Planets 122, 94–109. https://doi.org/10.1002/2016JE005132

Guidat, T., Pochat, S., Bourgeois, O., Souček, O., 2015. Landform assemblage in Isidis Planitia, Mars: Evidence for a 3 Ga old polythermal ice sheet. Earth Planet. Sci. Lett. 411, 253–267.

Gutiérrez-Santolalla, F., Acosta, E., Ríos, S., Guerrero, J., Lucha, P., 2005. Geomorphology and

geochronology of sackung features (uphill-facing scarps) in the Central Spanish Pyrenees. Geomorphology 69, 298–314. https://doi.org/10.1016/j.geomorph.2005.01.012

Haberle, R.M., Clancy, R.T., Forget, F., Smith, M.D., Zurek, R.W., 2017. The atmosphere and climate of Mars. Cambridge University Press.

Hambrey, M.J., 2004. Glaciers. Cambridge University Press Cambridge.

Hambrey, M.J., Huddart, D., Bennett, M.R., Glasser, N.F., 1997. Genesis of "hummocky moraines" by thrusting in glacier ice: evidence from Svalbard and Britain. J. Geol. Soc. 154, 623–632. https://doi.org/10.1144/gsjgs.154.4.0623

Harrison, K., Grimm, R., 2005. Groundwater-controlled valley networks and the decline of surface runoff on early Mars. J. Geophys. Res. Planets 110. https://doi.org/10.1029/2005JE002455

Harrison, K.P., Chapman, M.G., 2010. Episodic ponding and outburst flooding associated with chaotic terrains in Valles Marineris, in: Lakes on Mars, Edited by N.A. Cabrol and E.A. Grin. Elsevier B.V. ISBN 978-0444528544, 2010, P. 163-194. pp. 163–194.

Harrison, K.P., Chapman, M.G., 2008. Evidence for ponding and catastrophic floods in central Valles Marineris, Mars. Icarus 198, 351–364. https://doi.org/10.1016/j.icarus.2008.08.003

Hartmann, W.K., Neukum, G., 2001. Cratering Chronology and the Evolution of Mars, in: Chronology and Evolution of Mars, Space Sciences Series of ISSI. Springer, Dordrecht, pp. 165–194.

Head, J.W., Marchant, D.R., 2003. Cold-based mountain glaciers on Mars: Western Arsia Mons. Geology 31, 641–644. https://doi.org/10.1130/0091-7613(2003)031<0641:CMGOMW>2.0.CO;2

Head, J.W., Marchant, D.R., Agnew, M.C., Fassett, C.I., Kreslavsky, M.A., 2006. Extensive

valley glacier deposits in the northern mid-latitudes of Mars: Evidence for Late Amazonian obliquity-driven climate change. Earth Planet. Sci. Lett. 241, 663–671. https://doi.org/10.1016/j.epsl.2005.11.016

Head, J.W., Mustard, J.F., Kreslavsky, M.A., Milliken, R.E., Marchant, D.R., 2003. Recent ice ages on Mars. Nature 426, 797–802. https://doi.org/10.1038/nature02114

Head, J.W., Neukum, G., Jaumann, R., Hiesinger, H., Hauber, E., Carr, M., Masson, P., Foing, B., Hoffmann, H., Kreslavsky, M., 2005. Tropical to mid-latitude snow and ice accumulation, flow and glaciation on Mars. Nature 434, 346.

Head, J.W., Weiss, D.K., 2014. Preservation of ancient ice at Pavonis and Arsia Mons: tropical mountain glacier deposits on Mars. Planet. Space Sci. 103, 331–338.

Herkenhoff, K.E., Byrne, S., Russell, P.S., Fishbaugh, K.E., McEwen, A.S., 2007. Meter-Scale Morphology of the North Polar Region of Mars. Science 317, 1711–1715. https://doi.org/10.1126/science.1143544

Hubbard, B., Milliken, R.E., Kargel, J.S., Limaye, A., Souness, C., 2011. Geomorphological characterisation and interpretation of a mid-latitude glacier-like form: Hellas Planitia, Mars. Icarus 211, 330–346.

Hubbard, B., Souness, C., Brough, S., 2014. Glacier-like forms on Mars. The Cryosphere 8, 2047.

Hurowitz, J.A., Grotzinger, J.P., Fischer, W.W., McLennan, S.M., Milliken, R.E., Stein, N., Vasavada, A.R., Blake, D.F., Dehouck, E., Eigenbrode, J.L., Fairén, A.G., Frydenvang, J., Gellert, R., Grant, J.A., Gupta, S., Herkenhoff, K.E., Ming, D.W., Rampe, E.B., Schmidt, M.E., Siebach, K.L., Stack-Morgan, K., Sumner, D.Y., Wiens, R.C., 2017. Redox stratification of an ancient lake in Gale crater, Mars. Science 356, eaah6849.

https://doi.org/10.1126/science.aah6849

Ivanov, M.A., Head, J.W., 2001. Chryse Planitia, Mars: Topographic configuration, outflow channel continuity and sequence, and tests for hypothesized ancient bodies of water using Mars Orbiter Laser Altimeter (MOLA) data. J. Geophys. Res. 106, 3275–3296. https://doi.org/10.1029/2000JE001257

Jamieson, H.E., Robinson, C., Alpers, C.N., McCleskey, R.B., Nordstrom, D.K., Peterson, R.C., 2005. Major and trace element composition of copiapite-group minerals and coexisting water from the Richmond mine, Iron Mountain, California. Chem. Geol., Geochemistry of Sulfate Minerals: A tribute to Robert O. Rye 215, 387–405. https://doi.org/10.1016/j.chemgeo.2004.10.001

Jarman, D., 2006. Large rock slope failures in the Highlands of Scotland: Characterisation, causes and spatial distribution. Eng. Geol., Large Landslides: dating, triggering, modelling, and hazard assessment 83, 161–182. https://doi.org/10.1016/j.enggeo.2005.06.030

Johnson, P.L., Cotton, W.R., 2005. The Santiago Landslide and Associated Ridge-top Graben (Sackungen): Implications for Paleoseismic Landslide Studies. Environ. Eng. Geosci. 11, 5–15. https://doi.org/10.2113/11.1.5

Kleman, J., Hättestrand, C., 1999. Frozen-bed Fennoscandian and Laurentide ice sheets during the Last Glacial Maximum. Nature 402, 63. https://doi.org/10.1038/47005

Klingelhöfer, G., Morris, R.V., Bernhardt, B., Schröder, C., Rodionov, D.S., Souza, P.A. de, Yen, A., Gellert, R., Evlanov, E.N., Zubkov, B., Foh, J., Bonnes, U., Kankeleit, E., Gütlich, P., Ming, D.W., Renz, F., Wdowiak, T., Squyres, S.W., Arvidson, R.E., 2004. Jarosite and Hematite at Meridiani Planum from Opportunity's Mössbauer Spectrometer. Science 306, 1740–1745. https://doi.org/10.1126/science.1104653

Kowalewski, D.E., Marchant, D.R., Levy, J.S., Head, J.W., 2006. Quantifying low rates of summertime sublimation for buried glacier ice in Beacon Valley, Antarctica. Antarct. Sci. 18, 421–428. https://doi.org/10.1017/S0954102006000460

Kowalewski, D.E., Marchant, D.R., Swanger, K.M., Head III, J.W., 2011. Modeling vapor diffusion within cold and dry supraglacial tills of Antarctica: Implications for the preservation of ancient ice. Geomorphology 126, 159–173.

Kurokawa, H., Sato, M., Ushioda, M., Matsuyama, T., Moriwaki, R., Dohm, J.M., Usui, T., 2014. Evolution of water reservoirs on Mars: Constraints from hydrogen isotopes in martian meteorites. Earth Planet. Sci. Lett. 394, 179–185.

Lacelle, D., Léveillé, R., 2010. Acid drainage generation and associated Ca–Fe–SO4 minerals in a periglacial environment, Eagle Plains, Northern Yukon, Canada: A potential analogue for low-temperature sulfate formation on Mars. Planet. Space Sci., Exploring other worlds by exploring our own: The role of terrestrial analogue studies in planetary exploration 58, 509–521. https://doi.org/10.1016/j.pss.2009.06.009

Landis, M., Byrne Shane, Daubar Ingrid J., Herkenhoff Kenneth E., Dundas Colin M., 2016. A revised surface age for the North Polar Layered Deposits of Mars. Geophys. Res. Lett. 43, 3060–3068. https://doi.org/10.1002/2016GL068434

Laskar, J., Correia, A.C.M., Gastineau, M., Joutel, F., Levrard, B., Robutel, P., 2004. Long term evolution and chaotic diffusion of the insolation quantities of Mars. Icarus 170, 343–364. https://doi.org/10.1016/j.icarus.2004.04.005

Laskar, J., Levrard, B., Mustard, J.F., 2002. Orbital forcing of the martian polar layered deposits. Nature 419, 375. https://doi.org/10.1038/nature01066

Leask, H.J., Wilson, L., Mitchell, K.L., 2006. Formation of Aromatum Chaos, Mars:

Morphological development as a result of volcano-ice interactions. J. Geophys. Res. Planets 111, E08071. https://doi.org/10.1029/2005JE002549

Le Deit, L., Bourgeois, O., Mège, D., Hauber, E., Le Mouélic, S., Massé, M., Jaumann, R., Bibring, J.-P., 2010. Morphology, stratigraphy, and mineralogical composition of a layered formation covering the plateaus around Valles Marineris, Mars: Implications for its geological history. Icarus 208, 684–703. https://doi.org/10.1016/j.icarus.2010.03.012

Levy, J., Fassett Caleb I., Head James W., Schwartz Claire, Watters Jaclyn L., 2014. Sequestered glacial ice contribution to the global Martian water budget: Geometric constraints on the volume of remnant, midlatitude debris-covered glaciers. J. Geophys. Res. Planets 119, 2188–2196. https://doi.org/10.1002/2014JE004685

Lichtenberg, K., Arvidson Raymond E., Morris Richard V., Murchie Scott L., Bishop Janice L., Fernandez Remolar David, Glotch Timothy D., Noe Dobrea Eldar, Mustard John F., Andrews-Hanna Jeffrey, Roach Leah H., 2010. Stratigraphy of hydrated sulfates in the sedimentary deposits of Aram Chaos, Mars. J. Geophys. Res. Planets 115. https://doi.org/10.1029/2009JE003353

Liu, Y., Catalano, J.G., 2016. Implications for the aqueous history of southwest Melas Chasma, Mars as revealed by interbedded hydrated sulfate and Fe/Mg-smectite deposits. Icarus 271, 283–291. https://doi.org/10.1016/j.icarus.2016.02.015

Lucchitta, B.K., 1999. Geologic map of Ophir and central Candor Chasmata (MTM -05072) of Mars (USGS Numbered Series No. 2568), IMAP. U.S. Geological Survey, Reston, VA.

Lunine, J.I., Chambers, J., Morbidelli, A., Leshin, L.A., 2003. The origin of water on Mars. Icarus 165, 1–8.

Madeleine, J.-B., Forget, F., Head, J.W., Levrard, B., Montmessin, F., Millour, E., 2009.

Amazonian northern mid-latitude glaciation on Mars: A proposed climate scenario. Icarus 203, 390–405. https://doi.org/10.1016/j.icarus.2009.04.037

Makowska, M., Mège, D., Gueydan, F., Chéry, J., 2016. Mechanical conditions and modes of paraglacial deep-seated gravitational spreading in Valles Marineris, Mars. Geomorphology 268, 246–252. https://doi.org/10.1016/j.geomorph.2016.06.011

Mangold, N., Quantin, C., Ansan, V., Delacourt, C., Allemand, P., 2004. Evidence for Precipitation on Mars from Dendritic Valleys in the Valles Marineris Area. Science 305, 78–81. https://doi.org/10.1126/science.1097549

Marchant, D.R., Lewis, A.R., Phillips, W.M., Moore, E.J., Souchez, R.A., Denton, G.H., Sugden, D.E., Potter, N., Landis, G.P., 2002. Formation of patterned ground and sublimation till over Miocene glacier ice in Beacon Valley, southern Victoria Land, Antarctica. GSA Bull. 114, 718–730. https://doi.org/10.1130/0016-7606(2002)114<0718:FOPGAS>2.0.CO;2

Marra, W.A., McLelland, S.J., Parsons, D.R., Murphy, B.J., Hauber, E., Kleinhans, M.G., 2015. Groundwater seepage landscapes from distant and local sources in experiments and on Mars. Earth Surf. Dyn. 3, 389–408. https://doi.org/10.5194/esurf-3-389-2015

McCalpin, J.P., Irvine, J.R., 1995. Sackungen at the Aspen Highlands Ski Area, Pitkin County, Colorado. Environ. Eng. Geosci. I, 277–290. https://doi.org/10.2113/gseegeosci.I.3.277

McCauley, J.F., Carr, M.H., Cutts, J.A., Hartmann, W.K., Masursky, H., Milton, D.J., Sharp, R.P., Wilhelms, D.E., 1972. Preliminary mariner 9 report on the geology of Mars. Icarus 17, 289–327. https://doi.org/10.1016/0019-1035(72)90003-6

Mège, D., Bourgeois, O., 2011. Equatorial glaciations on Mars revealed by gravitational collapse of Valles Marineris wallslopes. Earth Planet. Sci. Lett. 310, 182–191. https://doi.org/10.1016/j.epsl.2011.08.030

Meresse, S., Costard, F., Mangold, N., Masson, P., Neukum, G., 2008. Formation and evolution of the chaotic terrains by subsidence and magmatism: Hydraotes Chaos, Mars. Icarus 194, 487–500. https://doi.org/10.1016/j.icarus.2007.10.023

Metz, J.M., Grotzinger, J.P., Mohrig, D., Milliken, R., Prather, B., Pirmez, C., McEwen, A.S., Weitz, C.M., 2009. Sublacustrine depositional fans in southwest Melas Chasma. J. Geophys. Res. Planets 114, E10002. https://doi.org/10.1029/2009JE003365

Michalski, J.R., Dobrea, E.Z.N., Niles, P.B., Cuadros, J., 2017. Ancient hydrothermal seafloor deposits in Eridania basin on Mars. Nat. Commun. 8, 15978. https://doi.org/10.1038/ncomms15978

Noe Dobrea, E.Z., 2006. Correlations Bewteen Sulfate and Hematite Deposits as Observed by OMEGA, in: Workshop on Martian Sulfates as Recorders of Atmospheric-Fluid-Rock Interactions. p. 61.

Noe Dobrea, E.Z., Poulet, F., Malin, M.C., 2008. Correlations between hematite and sulfates in the chaotic terrain east of Valles Marineris. Icarus 193, 516–534. https://doi.org/10.1016/j.icarus.2007.06.029

Nummedal, D., Prior, D.B., 1981. Generation of Martian chaos and channels by debris flows. Icarus 45, 77–86. https://doi.org/10.1016/0019-1035(81)90007-5

Okubo, C.H., 2016. Morphologic evidence of subsurface sediment mobilization and mud volcanism in Candor and Coprates Chasmata, Valles Marineris, Mars. Icarus 269, 23–37. https://doi.org/10.1016/j.icarus.2015.12.051

Okubo, C.H., Gaither, T.A., 2017. Bedrock and structural geologic maps of eastern Candor Sulci, western Ceti Mensa, and southeastern Ceti Mensa, Candor Chasma, Valles Marineris region of Mars (USGS Numbered Series No. 3359), Scientific Investigations Map. U.S.

Geological Survey, Reston, VA.

Okubo, C.H., McEwen, A.S., 2007. Fracture-Controlled Paleo-Fluid Flow in Candor Chasma, Mars. Science 315, 983–985. https://doi.org/10.1126/science.1136855

Pedersen, G.B.M., 2014. Chaotic Terrain (Mars), in: Encyclopedia of Planetary Landforms. Springer New York, New York, NY, pp. 1–6.

Pedersen, G.B.M., Head, J.W., 2011. Chaos formation by sublimation of volatile-rich substrate: Evidence from Galaxias Chaos, Mars. Icarus 211, 316–329. https://doi.org/10.1016/j.icarus.2010.09.005

Peulvast, J.P., Masson, P.L., 1993. Erosion and tectonics in Central Valles Marineris (Mars): a new morpho-structural model. Earth Moon Planets 61, 191–217. https://doi.org/10.1007/BF00572245

Quantin, C., Allemand, P., Delacourt, C., 2004a. Morphology and geometry of Valles Marineris landslides. Planet. Space Sci., Planet Mars. Sponsors: Centre National d'Etudes Spatiales (CNES); Centre National de la Recherche Scientifique (CNRS); Observatoire de Paris 52, 1011–1022. https://doi.org/10.1016/j.pss.2004.07.016

Quantin, C., Allemand, P., Mangold, N., Delacourt, C., 2004b. Ages of Valles Marineris (Mars) landslides and implications for canyon history. Icarus 172, 555–572. https://doi.org/10.1016/j.icarus.2004.06.013

Quantin, C., Allemand, P., Mangold, N., Dromart, G., Delacourt, C., 2005. Fluvial and lacustrine activity on layered deposits in Melas Chasma, Valles Marineris, Mars. J. Geophys. Res. Planets 110, E12S19. https://doi.org/10.1029/2005JE002440

Roach, L.H., Mustard, J.F., Lane, M.D., Bishop, J.L., Murchie, S.L., 2010. Diagenetic haematite and sulfate assemblages in Valles Marineris. Icarus 2, 659–674.

https://doi.org/10.1016/j.icarus.2009.11.029

Rodríguez, J.A.P., Kargel, J.S., Baker, V.R., Gulick, V.C., Berman, D.C., Fairén, A.G., Linares, R., Zarroca, M., Yan, J., Miyamoto, H., Glines, N., 2015. Martian outflow channels: How did their source aquifers form, and why did they drain so rapidly? Sci. Rep. 5, 13404. https://doi.org/10.1038/srep13404

Rodríguez, J.A.P., Kargel, J.S., Tanaka, K.L., Crown, D.A., Berman, D.C., Fairén, A.G., Baker, V.R., Furfaro, R., Candelaria, P., Sasaki, S., 2011. Secondary chaotic terrain formation in the higher outflow channels of southern circum-Chryse, Mars. Icarus 213, 150–194. https://doi.org/10.1016/j.icarus.2010.09.027

Rodríguez, J.A.P., Sasaki, S., Miyamoto, H., 2003. Nature and hydrological relevance of the Shalbatana complex underground cavernous system. Geophys. Res. Lett. 30, 1304. https://doi.org/10.1029/2002GL016547

Rodríguez, J.A.P., Zarroca, M., Linares, R., Gulick, V., Weitz, C.M., Yan, J., Fairén, A.G., Miyamoto, H., Platz, T., Baker, V., Kargel, J., Glines, N., Higuchi, K., 2016. Groundwater flow induced collapse and flooding in Noctis Labyrinthus, Mars. Planet. Space Sci. 124, 1–14. https://doi.org/10.1016/j.pss.2015.12.009

Rodriguez, J.A., Sasaki, S., Kuzmin, R.O., Dohm, J.M., Tanaka, K.L., Miyamoto, H., Kurita, K., Komatsu, G., Fairén, A.G., Ferris, J.C., 2005. Outflow channel sources, reactivation, and chaos formation, Xanthe Terra, Mars. Icarus 175, 36–57.

Rossi, A.P., Komatsu, G., Kargel, J.S., 2000. Rock Glacier-like Landforms in Valles Marineris, Mars. Presented at the Lunar and Planetary Science Conference.

Schultz, R.A., 1998. Multiple-process origin of Valles Marineris basins and troughs, Mars. Planet. Space Sci. 46, 827–834. https://doi.org/10.1016/S0032-0633(98)00030-0

Scott, D.H., Tanaka, K.L., 1986. Geologic map of the western equatorial region of Mars.

Sharp, R.P., 1973. Mars: Fretted and chaotic terrains. J. Geophys. Res. 78, 4073–4083. https://doi.org/10.1029/JB078i020p04073

Sharp, R.P., Soderblom, L.A., Murray, B.C., Cutts, J.A., 1971. The surface of Mars 2. Uncratered terrains. J. Geophys. Res. 76, 331–342. https://doi.org/10.1029/JB076i002p00331

Shean, D.E., Head, J.W., Fastook, J.L., Marchant, D.R., 2007. Recent glaciation at high elevations on Arsia Mons, Mars: Implications for the formation and evolution of large tropical mountain glaciers. J. Geophys. Res. Planets 112.

Shean, D.E., Head, J.W., Marchant, D.R., 2005. Origin and evolution of a cold-based tropical mountain glacier on Mars: The Pavonis Mons fan-shaped deposit. J. Geophys. Res. Planets 110, E05001. https://doi.org/10.1029/2004JE002360

Smith, D.E., Zuber, M.T., Solomon, S.C., Phillips, R.J., Head, J.W., Garvin, J.B., Banerdt, W.B., Muhleman, D.O., Pettengill, G.H., Neumann, G.A., Lemoine, F.G., Abshire, J.B., Aharonson, O., David, C., Brown, Hauck, S.A., Ivanov, A.B., McGovern, P.J., Zwally, H.J., Duxbury, T.C., 1999. The Global Topography of Mars and Implications for Surface Evolution. Science 284, 1495–1503. https://doi.org/10.1126/science.284.5419.1495

Squyres, S.W., Grotzinger, J.P., Arvidson, R.E., Bell, J.F., Calvin, W., Christensen, P.R., Clark, B.C., Crisp, J.A., Farrand, W.H., Herkenhoff, K.E., Johnson, J.R., Klingelhöfer, G., Knoll, A.H., McLennan, S.M., McSween, H.Y., Morris, R.V., Rice, J.W., Rieder, R., Soderblom, L.A., 2004. In Situ Evidence for an Ancient Aqueous Environment at Meridiani Planum, Mars. Science 306, 1709–1714. https://doi.org/10.1126/science.1104559

Squyres, S.W., Knoll, A.H., 2005. Sedimentary rocks at Meridiani Planum: Origin, diagenesis, and implications for life on Mars. Earth Planet. Sci. Lett. 240, 1–10.

https://doi.org/10.1016/j.epsl.2005.09.038

Stuurman, C.M., Osinski, G.R., Holt, J.W., Levy, J.S., Brothers, T.C., Kerrigan, M., Campbell, B.A., 2016. SHARAD detection and characterization of subsurface water ice deposits in Utopia Planitia, Mars. Geophys. Res. Lett. 43, 9484–9491.

Sweeney, J., Warner, N.H., Ganti, V., Golombek, M.P., Lamb, M.P., Fergason, R., Kirk, R., 2018. Degradation of 100-m-Scale Rocky Ejecta Craters at the InSight Landing Site on Mars and Implications for Surface Processes and Erosion Rates in the Hesperian and Amazonian. J. Geophys. Res. Planets 123, 2732–2759. https://doi.org/10.1029/2018JE005618

Thaisen, K.G., Schieber, J., Dumke, A., Hauber, E., Neukum, G., 2008. Geomorphic Evidence for Significant Glacial and Fluvial Activity in Candor Chasma, Mars. Presented at the Lunar and Planetary Science Conference, p. 2358.

Thollot, P., Mangold, N., Ansan, V., Le Mouélic, S., Milliken, R.E., Bishop, J.L., Weitz, C.M., Roach, L.H., Mustard, J.F., Murchie, S.L., 2012. Most Mars minerals in a nutshell: Various alteration phases formed in a single environment in Noctis Labyrinthus. J. Geophys. Res. Planets 117, E00J06. https://doi.org/10.1029/2011JE004028

Tosca, N.J., McLennan, S.M., Clark, B.C., Grotzinger, J.P., Hurowitz, J.A., Knoll, A.H., Schröder, C., Squyres, S.W., 2005. Geochemical modeling of evaporation processes on Mars: Insight from the sedimentary record at Meridiani Planum. Earth Planet. Sci. Lett., Sedimentary Geology at Meridiani Planum, Mars 240, 122–148. https://doi.org/10.1016/j.epsl.2005.09.042

Varnes, D.J., Radbruch-Hall, D.H., Savage, W.Z., 1989. Topographic and Structural Conditions in Areas of Gravitational Spreading of Ridges in the Western United States. U. S. Geol. Surv. Prof. Pap. USA 1496.

Villanueva, G.L., Mumma, M.J., Novak, R.E., Käufl, H.U., Hartogh, P., Encrenaz, T., Tokunaga,

A., Khayat, A., Smith, M.D., 2015. Strong water isotopic anomalies in the martian atmosphere:

Probing current and ancient reservoirs. Science 348, 218–221.

https://doi.org/10.1126/science.aaa3630

Waller, R.I., 2001. The influence of basal processes on the dynamic behaviour of cold-based

glaciers. Quat. Int. 86, 117–128.

Warner, N., Gupta, S., Lin, S.-Y., Kim, J.-R., Muller, J.-P., Morley, J., 2010. Late Noachian to

Hesperian climate change on Mars: Evidence of episodic warming from transient crater lakes

near Ares Vallis. J. Geophys. Res. Planets 115, E06013. https://doi.org/10.1029/2009JE003522

Warner, N., Gupta, S., Muller, J.-P., Kim, J.-R., Lin, S.-Y., 2009. A refined chronology of

catastrophic outflow events in Ares Vallis, Mars. Earth Planet. Sci. Lett. 288, 58–69.

Warner, N.H., Gupta, S., Kim, J.-R., Muller, J.-P., Le Corre, L., Morley, J., Lin, S.-Y.,

McGonigle, C., 2011. Constraints on the origin and evolution of Iani Chaos, Mars. J. Geophys.

Res. Planets 116, E06003. https://doi.org/10.1029/2010JE003787

Warner, N.H., Sowe, M., Gupta, S., Dumke, A., Goddard, K., 2013. Fill and spill of giant lakes

in the eastern Valles Marineris region of Mars. Geology 41, 675–678.

https://doi.org/10.1130/G34172.1

Weitz, C.M., Irwin III, R.P., Chuang, F.C., Bourke, M.C., Crown, D.A., 2006. Formation of a

terraced fan deposit in Coprates Catena, Mars. Icarus 184, 436–451.

https://doi.org/10.1016/j.icarus.2006.05.024

Wendt, L., Gross, C., Kneissl, T., Sowe, M., Combe, J.-P., LeDeit, L., McGuire, P.C., Neukum,

G., 2011. Sulfates and iron oxides in Ophir Chasma, Mars, based on OMEGA and CRISM

observations. Icarus 213, 86–103. https://doi.org/10.1016/j.icarus.2011.02.013

Wordsworth, R.D., Kerber, L., Pierrehumbert, R.T., Forget, F., Head, J.W., 2015. Comparison of

"warm and wet" and "cold and icy" scenarios for early Mars in a 3-D climate model. J. Geophys. Res. Planets 120, 2015JE004787. https://doi.org/10.1002/2015JE004787

Zegers, T.E., Oosthoek, J.H.P., Rossi, A.P., Blom, J.K., Schumacher, S., 2010. Melt and collapse of buried water ice: An alternative hypothesis for the formation of chaotic terrains on Mars. Earth Planet. Sci. Lett. 297, 496–504. https://doi.org/10.1016/j.epsl.2010.06.049